

Conceptual representation of fluid flow conditions associated with faults in sedimentary basins

Project: Research to improve treatment of faults and aquitards in Australian regional groundwater models to improve assessment of impacts of CSG extraction

Prepared for the Department of the Environment and Energy.

2018



Research Team

Jim Underschultz¹, Joan Esterle¹, Julian Strand² and Susan Hayes¹

1: The University of Queensland

2: CSIRO

Acknowledgements

The authors would like to thank A. Garnett, K. Barbosa and H. Schultz at the University of Queensland for internal review, Ryan Morris of Origin Energy for an industry review, Dirk Mallants of CSIRO for a contractors review and Alistair Usher of the Department of the Environment and Energy for a client review. These reviews have strengthened the reports technical content and readability.

Disclosure/Disclaimer

The UQ, Centre of Coal Seam Gas is currently funded by the University of Queensland 22% (\$5 million) and the Industry members 78% (\$17.5 million) over 5 years. An additional \$3.0 million is provided by industry members for research infrastructure costs. The industry members are QGC, Santos, Arrow and APLNG. The centre conducts research across Water, Geoscience, Petroleum Engineering and Social Performance themes.

For more information about the Centre's activities and governance see: <http://www.ccsq.uq.edu.au/>

Researchers within or working with the Centre for Coal Seam Gas are bound by the same policies and procedures as other researchers within The University of Queensland, which are designed to ensure the integrity of research. You can view these policies at: <http://ppl.app.uq.edu.au/content/4.-research-and-research-training>

The Australian Code for the Responsible Conduct of Research outlines expectations and responsibilities of researchers to further ensure independent and rigorous investigations.

This report has been peer reviewed.

Citation

This report should be cited as:

Underschultz, J., Esterle, J., Strand, J. and Hayes, S. (2018). Conceptual representation of fluid flow conditions associated with faults in sedimentary basins. Prepared for the Department of the Environment and Energy by The University of Queensland Centre for Coal Seam Gas, Queensland. 61 p.

About this report

This report forms Milestone 3, Deliverable 2A of the DOEE funded project 'Research to improve treatment of faults and aquitards in Australian regional groundwater models to improve assessment of impacts of CSG extraction'.

The deliverable requirements for this document are: "DOEE report with conceptual representations of different groundwater flow conditions associated with faults in sedimentary basins, including their influence on connectivity within individual formations, between formations, and between groundwater and surface water environments".

The report has been compiled by The University of Queensland, Centre for Coal Seam Gas in collaboration with CSIRO.

Document Control Sheet

File name: Deliverable2.2_Conceptual_Flow_and_Faults_DraftV1.2

Version #	Date Distributed	Reviewed By	Revision Date	Brief description of changes
1.0	1-06-2015	J Strand: CSIRO A Garnet: UQ J Esterle: UQ	29-05-2015	Report structure Context setting added Referencing
1.1	16-06-2015	S. Hayes: UQ K. Barbosa: UQ	16-06-2015	General editorial Report Formatting
1.1		Dirk Mallants: CSIRO	Review received 20-06-2015	Modified descriptions of physical processes. Sharper images for figures Summary table re: implications for regional GW models added
1.1	[15-07-2015]	Alistair Usher(Office of Water Science) and Ryan Morris (Origin)	Review received 15-07-2015 Revised on 05-08- 2015	Major report revision and added section on springs and faults
1.2	[1-08-15]	Joan Esterle and Julian Strand	12-08-2015	Revise report
1.3	13-08-2015	Dirk Mallants: CSIRO	Review received 14-10-2015	Update Acronyms, Glossary & Symbols Added further discussion to demonstrate relevance for groundwater modelling Technical clarifications
1.3	15-10-2015	Susan Hayes: UQ		Formatting and editorial including references
1.4	01-11-2015	Dirk Mallants Susan Hayes Julian Strand and Joan Esterle		Need to standardise this report with the sister report: glossary and other components and ensure that there was consistency in content and style between the two report
1.5	21-12-2015	Jim Underschultz	23-12-2015	1 st Final report revision
1.6	24-12-2015 22-01-2016	Dirk Mallants Scott Lawson	12-01-2016 03-02-2016	Final editorial overview Jim's 2 nd Final report version

Executive Summary

The project *“Research to improve treatment of faults and aquitards in Australian regional groundwater models to improve assessment of impacts of CSG extraction”* focuses on identifying and assessing technical uncertainty with deep groundwater extraction and depressurisation associated with energy resources development. The project aims to develop methodologies and techniques that will improve the predictive capability of regional groundwater models used in this context. The project has three components: 1) examination of aquitards, 2) examination of faults, and 3) examination of upscaling aquitard and fault properties such that they can be adequately represented in regional groundwater flow models. This report represents the literature review related to part 2 on faults. The overview provides the framework that can be used to guide research into appropriate methodologies and procedures of aquitard and fault zone representation in regional groundwater models.

There is an extensive body of scientific literature on fault characteristics and their genesis in structural geology journals, however, the understanding of fault hydraulic properties and their transmission (or not) of fluids in sedimentary sequences primarily comes from two domains of research: 1) conventional oil and gas exploration and production geology where faults can either allow hydrocarbons to accumulate in commercial volumes, or to leak rendering an otherwise valid trap to be “dry” or sub-economic, and 2) hydrogeological and ecological research on groundwater springs occurring along faults that come to surface. The economic imperative of having pre drill-predictive capability in estimating fault seal capacity to conventional hydrocarbons accumulations has led to the development of several procedures and techniques that evaluate various aspects of fault zone hydraulic characteristics at various in-situ environmental conditions (pressure, temperature, stress, wettability). These include: fault zone architecture and juxtaposition analysis, mechanical seal capacity and fault reactivation potential, capillary fault seal capacity and hydrodynamic analysis, and sub-seismic strain analysis. The oil and gas industry uses field production history and observed field compartmentalisation to calibrate and validate methodologies for predicting fault seal capacity and the representative hydraulic parameters of fault zones. In the domain of groundwater hydrogeology, surface water hydrology and ecology, observations of groundwater spring temperature, flux and geochemical characteristics for springs occurring along faults are used to infer fault zone hydraulic properties.

From this literature review and assessment of commonly used fault analysis methodology, we collected several case study examples of fault systems and their hydraulic behaviour and make the following general observations:

- Faults can exhibit the full range of hydraulic characteristics between providing a hydraulic barrier sufficient to trap hydrocarbons for millions of years to being a conduit with transmissivities capable of transmitting groundwater from depth to surface thermal springs;
- Faults can exhibit different hydraulic properties at different locations on the fault plane;
- The hydraulic behaviour exhibited by faults is related to a combination of: 1) the geometry or architecture of the fault complex, 2) the rheology of the host rocks that the fault plane crosses, and 3) the distribution and orientation of in situ stress;
- Faults occur in predictable populations representing a power law distribution of fault size (or throw). The observed strain together with the predicted fault size distribution can be used to estimate the unobserved (sub-seismic) strain;
- In scenarios of coal seam gas development where the formation pressure is reduced regionally over time by groundwater abstraction associated with gas production, there is an associated change in the effective stress and thus potential for a change in the sealing properties of faults. Coupled geomechanical and hydrodynamic processes are required to characterise these transient processes;
- Fault hydraulic properties can depend on the environmental conditions (pressure, temperature, depth and stress) both at the time the fault formed and the present day; and
- Observations of springs occurring along faults including the flux of spring discharge, temperature and geochemistry can be used to calibrate and validate the hydraulic characteristics estimated for fault zones.

Concerns of aquifer pressure depletion, fugitive methane migration and degradation of aquifer water quality due to CSG development effects propagating up faults can be investigated through the use of regional groundwater models, if they are appropriately parameterised. A key aspect of this investigative approach is to develop and parameterise regional groundwater models that accurately represent the properties of the rock framework and its contained fluids. In this review we consider methodologies for estimating the properties of faults and how these can be represented in regional groundwater models. There are a number of key parameters and processes that need to be assessed at a detailed scale and then up-scaled for parameterisation of regional models. For the incorporation of fault properties these include:

- Details of the host rock facies distributions and lithologies;
- Details of the fault throw distributions;
- Details of the in situ stress distribution;
- Details of the fault zone damage zone distribution and fault core distribution;
- Details of the mechanical strength of the fault plane and damage zone;
- Details of the host rock rheology, depth, temperature and how these relate to the tectonic and burial history (this is important for both the aquifer and aquitard layers transected by the fault);
- Details of the fluid pressure distribution in both the aquifers and aquitards on either side of the fault;
- Details of the various fluid types, densities, surface tensions and wettabilities;
- Details of other supporting fluid data such as formation water chemistry and formation temperature;
- Details of the transient nature of predicted reservoir and adjacent aquifer pressure depletion that could impact the effective stress; and
- Well characterised analogues from outcrop or sub-surface features that can be used to interpolate key characteristics not well enough constrained by data at the site location of interest.

This review provides the framework that can be used to guide research into appropriate methodologies and procedures of fault zone hydraulic characterization applied to regional groundwater models. Throughout the report available methods for the quantification of models and prediction of uncertainty are highlighted. It should be noted that the focus of the report is on groundwater flow and hydraulic responses; therefore the simulation of solute transport is not discussed.

Table of Contents

1	Introduction.....	19
2	Context	19
3	Assumptions and Methodology.....	20
4	Definitions and Terminology	21
5	Fault Zone Physical Characteristics.....	22
5.1	Fault Zone Architecture and in-Situ Stress.....	22
5.2	Mechanical Seal Capacity of Faults and Fault Reactivation	25
5.3	Sub-Seismic Strain	27
5.4	Permeability of Faults, Across Fault Leakage and Capillarity	30
5.4.1	Juxtaposition	31
5.4.2	Shale Gouge Ratio (SGR)	32
6	Movement of Fluids in Faulted Rocks.....	33
6.1	Multi-Phase Fluids and Capillarity	34
6.2	Consideration of Aquitards that are Hydrocarbon Wetting.....	37
7	Case Studies and Conceptual Flow Models in Faulted Rock.....	38
8	Groundwater Springs and Faults	48
9	More Detailed Fault Representations.....	48
10	Discussion and Summary of Fault Assessment, Sealing Capacity and Reactivation Potential	53
11	Implications for up-scaling to Regional Groundwater Models	54
12	References	56

List of Figures

Figure 1. Fault style sketches showing the principal stress axes and slip classifications of various faults. Note that in theory all faults have a certain amount of rotational component because displacement, even in a dip-slip fault, varies along the fault length. However, in a rotational fault the variation is greater between two nearby points along the fault strike than can be accounted for simply by the fault plane geometry. (Sorkhabi, 2013).....	23
Figure 2. Schematic diagram showing evolutionary stages of a relay ramp. Tick marks on the map view depict the down-thrown block of normal faults. (a) Stage I: the faults do not interact. (b) Stage II: the faults have started to interact and a relay ramp has developed to transfer the displacement among the segments. (c) Stage III: accumulated strain in the relay ramp has resulted in initiation of fracturing. (d) Stage IV: the relay ramp is broken by a breaching fault to form a single fault zone with strike irregularity. (e) Upper bench is abandoned and two segments joined through breaching of lower ramp that form an along-strike bend on the course of the main fault. Ciftci and Bozkurt (2007) modified from Peacock & Sanderson (1994).	24
Figure 3. A photo of a relay ramp between ~8cm displacement normal fault segments in the Liassic limestones and shales of Kilve, Somerset, UK (Fault Analysis Group, Dublin).	24
Figure 4. Conjugate fault system exposed in a 60 m high vertical cliff section of Liassic Limestone, Nash Point, South Wales. From Watterson et al. (1998) and images provided by Fault Analysis Group, Dublin ¹	25
Figure 5. (a) Graphical representation of the FAST method for risking the likelihood of fault reactivation using a Mohr-Coulomb diagram (after Mildren et al., 2002). The smaller the ΔP values (difference between effective stress and the failure criteria), the higher the risk of reactivation. (b) Polar plot showing the distribution of ΔP values for poles to fault planes from the Pyrenees-Macedon oil and gas fields. The highest risk of reactivation (lowest ΔP ; dark red) is on steeply dipping faults striking 060° and 120°, and E–W faults dipping at 60° (Bailey et al. 2006).	26
Figure 6. Schematic representation of typical fault reactivated trap geometries and their predicted oil column preservation characteristics. Arrows depict hydrocarbon leakage along high strain faults above the critical fault-horizon intersections. Note how certain faults are “sheltered” by reactivation of other nearby faults (Gartell et al. 2005).	28
Figure 7. Plot of multiple global data sets showing maximum displacement (d_{max}) against fault length (L) for normal faults (Kim & Sanderson, 2005).	29
Figure 8. Power law distribution of fault population throws at the SW Hub proposed carbon storage site in Western Australia: Perth Basin (Langhi et al. 2013).	30
Figure 9. Schematic diagram of various juxtaposition orientations (Neele et al. 2012).	31
Figure 10. An example of an Allan diagram (left) that shows across fault juxtaposition of multiple stacked and folded sandstone reservoir layers. the resulting across fault hydraulic communication controls the hydrocarbon spill points and hydrocarbon column heights. The plan view of the same structure (right) shows the trap geometry relative to the fault trace (Allan, 1989).	32
Figure 11. Example of shale gouge ratio method of calculation (Yielding et al., 1997) where V_{sh} is the volume of shale expressed as a % of clay minerals in a discrete bed thickness (Δz) and T is the fault throw.	33
Figure 12. Schematic presentation of a fault zone at its capillary seal capacity (A) trapping a hydrocarbon pool. B and C depict a zoom in of the fault zone-reservoir interface under different hydrodynamic conditions with a corresponding capillary pressure curve of the fault rock in question. The rock properties of the reservoir and fault seal are constant but the total seal capacity (P_{tc}) is demonstrated to change where in B) the hydrocarbon is pooled on the high hydraulic head side of the fault, and in C) the hydrocarbon is pooled on the low hydraulic head side of the fault (Underschultz and Strand, 2016).	35
Figure 13. Pressure-Depth plot with a hydrocarbon column equal to top seal P_t . In this case P_t is estimated to be the difference in the hydrocarbon and water pressure at the top of the column. ΔP is the equivalent pressure difference between H_w on either side of the seal (after Rodgers, 1999).	37
Figure 14. A schematic capillary pressure graph plotted against water saturation for both a typical reservoir (solid curve) and seal rock (dashed curve). P_{ce} is the capillary entry pressure and P_t is the threshold pressure. S_{wi} is irreducible water saturation.	37

Figure 15. Schematic fault hydrodynamics (modified from Otto et al., 2001). (a) Hydraulic head distributions in two stacked aquifers connected by a crosscutting conduit fault; (b) cross section of the conduit fault in (a) with upfault flow, and the corresponding pressure-elevation plot of WLT data from the two aquifers at the well location (Underschultz et al. 2005).	40
Figure 16. Hydraulic head in the Challis aquifer supporting the Challis hydrocarbon accumulation on Australia's North West Shelf. Blue contours are fresh water hydraulic head (m), orange arrows represent flow directions, pink dashed lines represent fault traces, the black line is the approximate edge of the oil pool with an oil water contact at ~-1417m elevation, green dots are oil wells and blue dots are wells with formation water recovery (Unpublished Underschultz et al. CSIRO IPETS consortia).	40
Figure 17. Schematic fault hydrodynamics (modified from Otto et al., 2001). (a) Hydraulic head distributions in two stacked aquifers crosscut by a barrier fault; and (b) cross section of the barrier fault in (a) with no upfault flow and the corresponding pressure-elevation plot of WLT data from the two aquifers at the well location. Underschultz et al. (2005)	41
Figure 18. Schematic cross section across a sealing fault with a theoretical hydraulic head distribution (black contours lines) in this dimension. Flow paths are marked with arrows. The bulk of the flux is likely occurring perpendicular to the line of section because the fault zone has a very low permeability resulting in the tight hydraulic head gradient.	42
Figure 19. Fresh-water hydraulic head (m) distribution for the Plover aquifer system, Vulcan Sub-basin (Underschultz et al. 2002).	43
Figure 20. Hydraulic head distribution map for the Barrow aquifer for the P–M fields. Inset shows alternative interpretation for head distribution in the compartment between Pyrenees-2 and West Muiron-5. Grey shading that define the contours representing fresh water hydraulic head (m). Heavy black lines represent major fault traces (Bailey et al. 2006).	44
Figure 21. A schematic diagram of the main features of a structural relay ramp (Di Bucci et al. 2006).	44
Figure 22. Detail of the model showing the groundwater flow patterns (black lines with arrows) around the fault relay. Contour interval is 10m (Bense and Van Balen 2004).	45
Figure 23. Hydraulic head in a shallow aquifer of the Lower Rhine Embayment of the Roer Valley Graben. Contour lines are fresh water hydraulic head (m) and heavy black lines with tick marks are major fault traces. Well locations are indicated by open circles (Bense and Van Balen, 2004).	45
Figure 24. Hydraulic head (m) distribution for the Mississippian aquifer western Canada (Underschultz et al. 2005). The white line in the SE corner of the map is the location of the cross section depicted in Figure 25 to follow.	46
Figure 25. Schematic strike cross section of the Brazeau thrust sheet (Underschultz et al. 2005, based on Begin and Spratt, 2002) the location of which is marked by a white line in the SE corner of Figure 24.	47
Figure 26. Shallow Fault zone with A) water level scenarios, and B) and C) negative and positive thermal anomalies respectively. (Bense et al. 2013).	47
Figure 27. Complex fault zone hydrogeology for a shallow aquifer horizon where A) shows surface focused investigations and B) shows subsurface focused investigations (Bense et al. 2013).	49
Figure 28. Complex fault zone hydrogeology for an aquifer horizon where A) is a block model, B) is a detailed scan through one fault core, C) is a detailed scan line through three fault cores, D) is the fracture density and permeability distribution on scan line B, E) is the fracture density and permeability distribution on scan line C, and F) categorisation matrix of damage zone width vs. permeability of fault core into flow characteristics (Bense et al. 2013).	50
Figure 29. Complex fault zone hydrogeology for an interbedded sequence of aquifers and aquitards where A) unlithified siliciclastic rheology, B is lithified siliciclastic rheology, C is crystalline rock rheology, and D) is carbonate rock rheology (Bense et al. 2013).	51
Figure 30. Fluid flow in fault zones from an active rift. Geometry of the detailed fault zone architecture related to the flux distribution of formation water where low to moderate ($<5 \times 10^3 \text{ m}^3/\text{s}$) and high ($>5 \times 10^3 \text{ m}^3/\text{s}$) flow rates shown by light and dark blue shading, respectively. The red dots show location and direction and relative rate of flow (Seebeck et al. 2014).	51
Figure 31. Fluid flow in fault zones from an active rift. Geometry of the detailed fault zone architecture related to the fracture density, permeability and flux distribution of formation water (Seebeck et al. 2014).	52

Figure 32. Typical architectural and structural elements of fault zones (Loveless et al. 2011). a) Fault zone in crystalline rocks (e.g. Caine et al., 1996) with a fault core (FC) and damage zone (DZ). b) Fault zone in poorly lithified sediment (e.g. Heynekamp et al., 1999; Rawling and Goodwin, 2003; Rawling and Goodwin, 2006), the mixed zone (MZ) is a third architectural element. 53

Abbreviations table

Abbreviation	Description
AE	Arrow Energy
APLNG	Australia Pacific Liquid Natural Gas
BTEX	Benzene, toluene, ethylbenzene and xylene
CBM	Coal bed methane
CSG	Coal seam gas
CSIRO	Commonwealth Scientific and Industrial Research Organisation
CSP	Clay Smear Potential
DNAPL	Dense non-aqueous phase liquid
DoE	Department of the Environment
DST	Drill Stem Test
FAST	Fault Analysis Software Tool
FLAC	Fast Lagrangian Analysis of Continua
FWL	Free Water Level
GAB	Great Artesian Basin
IESC	Independent Expert Scientific Committee on Coal Seam Gas and Large Coal Mining Development
IPETS	Integrated Predictive Evaluation of Traps and Seals
MDT	Modular Dynamic Test
MICP	Mercury Injection Capillary Pressure
NAPL	Non-aqueous phase liquid, such as petroleum
NSW	New South Wales
NW	North West
OWC	Oil-water contact
POWC	Present oil-water contact
QGC	Queensland Gas Company
QWC	Queensland Water Commission
RFT	Repeat Formation Test
SE	South East
SGR	Shale Gouge Ratio
SSF	Shale Smear Factor
SW	South West
WLT	Wireline Test

Symbols table

Symbol	Short description
ΔP	Excess pressure
ΔP_f	Across fault pressure difference
$\Delta \rho$	In situ density difference between hydrocarbon and formation water
Δz	Sedimentary bed thickness
C_f	Critical fracture density
g	Acceleration due to gravity
H_w	Hydraulic head calculated using water density
h	Hydrocarbon column height
k_{rw}	Relative permeability to water
k_{fz}	Fault zone permeability
k_{res}	Reservoir permeability
k_{ts}	Top seal permeability
P	Formation pressure
P_c	Capillary pressure of non-wetting phase
P_{ce}	Capillary entry pressure
P_t	Threshold pressure
P_{tc}	Total capillary seal capacity
S_h	Non-wetting phase saturation
S_g	Gas saturation
S_w	Water saturation
S_{wi}	Irreducible water saturation
T	Throw at a particular location on a fault surface
V_{sh}	Volume of shale expressed as a % of clay minerals within a given bed thickness

Glossary

Term	Description
Anisotropic	Having different physical properties in different directions.
Aquiclude	An impermeable body of rock or stratum of sediment that acts as a barrier to the flow of water.
Aquifer	A body of rock or stratum of sediment which is saturated and sufficiently permeable to transmit useful quantities of water to wells and springs.
Aquitard	A saturated body of rock or stratum of sediment that is less permeable than an aquifer and incapable of transmitting useful quantities of water. Aquitards often form a confining layer over an artesian aquifer.
Artesian	Groundwater with a hydraulic head above ground level.
Azimuth	The horizontal angle of an observer's bearing, measured clockwise from a reference direction such as true north.
Baseline survey	A survey carried out prior to any disturbance to determine the natural background levels of certain substances.
Buoyancy	Within the earth's gravitational field a buoyancy force is exerted when two different density fluids occur in the pore space of rocks where the lighter fluid experiences an upwards force and the denser fluid experiences a downward force.
Breccia	A rock composed of broken fragments of rock or minerals.
Calibration	The process of finding a relationship between two unknown (when the measurable quantities are not given a particular value for the amount considered or found a standard for the quantity) quantities. When one of quantity is known, which is made or set with one device, another measurement is made as similar way as possible with the first device using a second device. The measurable quantities may differ in two devices which are equivalent. The device with the known or assigned correctness is called the standard. The second device is the unit under test.
Calliper logs	A calliper log is a well logging tool that provides a continuous measurement of the size and shape of a borehole along its depth.
Capillary leakage	The flux of non-wetting fluid that has overcome the capillary threshold pressure and migrated across a sealing rock layer.
Capillary seal	A rock layer with sufficiently low permeability as to provide a capillary barrier to the upwards migration of a non-wetting fluid phase.
Cataclastic material	Rock fragments that has been wholly or partly formed by the progressive fracturing and comminution of existing rock, a process known as cataclasis, and is mainly found associated with fault zones.
CH ₄	Methane.
Coal measures	Geological strata containing multiple coal horizons or seams.
Coal seam	A coal seam is a single layer or bed of coal (sedimentary rock).
Coal seam gas	A form of natural gas (generally 95 to 97% methane, CH ₄) typically extracted from permeable coal seams at depths of 300 to 1000 m. Also called coal seam methane (CSM) or coalbed methane (CBM).
Coalesced	(Fault plane) multiple faults merging into one.
Compressive stress	The <i>stress</i> on materials under compression that leads to a smaller volume.
Confined aquifer	An aquifer that is isolated from the atmosphere by an aquitard or aquiclude. Pressure in confined aquifers is generally greater than atmospheric pressure.

Conventional gas	Conventional reservoirs are where gas is trapped by the buoyancy of the hydrocarbon phase beneath a low permeability seal and with a downdip formation water leg. In such cases a discrete hydrocarbon pool or field can be defined.
Coupled modelling	The process by which one numerical simulation solves one set of governing equations and then uses the answer in a second numerical simulation solving a different set of governing equations. For example a rock mechanical model may determine permeability in a given stress state and this permeability is used in a fluid dynamic model which calculates a change in pressure resulting in a new stress state. This new stress state results in a new permeability and so on.
Dense Non-Aqueous Phase Liquid	A liquid not miscible with water and denser than water.
Depressurisation	The lowering of static groundwater levels through the partial extraction of available groundwater, usually by means of pumping from one or several bores or wells.
Dilatancy Potential	The likelihood that a fracture might dilate in a given stress field.
Dilatant fault	A fault oriented relative to the stress field such that it is dilatant.
Discharge	An aquifer that has a flux to subcrop or the land surface. This may be expressed as a spring or base flow to surface drainage.
Effective stress	Total stress minus pore pressure.
En-echelon (fault)	Closely-spaced, parallel or subparallel, overlapping or step-like minor structural features in rock (faults, tension fractures), which lie oblique to the overall structural trend.
Fault damage zone	<p>Damage Zones are a result of brittle deformation along a fault zone where rocks are ground and crack in various orientations in response to stress. Some structures in damage zones are:</p> <ul style="list-style-type: none"> • Wing Cracks—Extension fractures associated with small amounts of displacement; • Horsetail Splay—Occur along larger faults and create a series of secondary pinnate shear fractures; • Synthetic Branch Faults—When deformation at a fault tip causes shear of the same sense of the motion of the fault; and • Antithetic Faults—when deformation at a fault tip causes shear of the opposite sense as the main fault. This creates rotation of the block in the damage zone.
Fault seal	A fault with sufficiently low permeability that it can trap hydrocarbons over geological time.
Fault throw	The vertical component of dip separation.
Flowback water	The initial flow of water returned to a well after fracture stimulation and prior to production.
Formation pressure	The fluid pressure measured at a point in an aquifer.
Formation water	Naturally occurring water that occurs in the sub-surface rock framework.
Fugitive methane	Methane released to the atmosphere by anthropogenic means.
Geochemistry	The interactive chemistry between formation water and rock mineralogy
Geomechanical analysis	The study of rock mechanics and stress.
Gouge	Unconsolidated tectonite (a rock formed by tectonic forces) with a very small grain size.

Groundwater	Water occurring naturally below ground level (whether in an aquifer or other low-permeability material), or water occurring at a place below ground that has been pumped, diverted or released to that place for storage. This does not include water held in underground tanks, pipes or other works
HCO ₃	Bicarbonate
Horner analysis	For time series data that approach an equilibrium (for example pressure increase with time on a shut in after pumping), a Horner analysis technique uses extrapolation to estimate the equilibrium value.
Hydraulic fracturing	Also known as 'fracking', 'fraccing' or 'fracture stimulation', is one process by which hydrocarbon (oil and gas) bearing geological formations are 'stimulated' to enhance the flow of hydrocarbons and other fluids towards the well. The hydraulic fracturing process involves the injection of fluids, gas, proppant and other additives under high pressure into a geological formation to create a conductive fracture. The fracture extends from the well into the reservoir, creating a large surface area through which gas and water are produced and then transported to the well via the conductive propped fracture channel.
Hydraulic gradient	The change in hydraulic head between different locations within or between aquifers or other formations, as indicated by bores constructed in those formations.
Hydraulic head	$(1) H_w = (P/\rho_w g) + Z$ <p> H_w = Hydraulic Head P = Formation Pressure ρ_w = Formation water density g = Acceleration of Gravity Z = Pressure Gauge Elevation </p>
Hydrochemical analysis	The analytical results of measuring ionic constituents and other attributes of a water sample.
Hydrodynamic analysis	The study of groundwater or formation water
Hydrodynamic processes	Geochemical, geomechanical, and hydraulic processes associated with groundwater or formation water systems.
In-situ stress	The stress at a point in the sub-surface.
Irreducible water saturation	The fraction of the pore space occupied by water when the hydrocarbon content is at maximum.
Isotope	Atoms that have the same number of protons but different numbers of neutrons are called isotopes. The element hydrogen, for example, has three commonly known isotopes: protium, deuterium and tritium
Juxtaposition analysis	An assessment of the strata located directly across a fault plane from one another.
Kinematic analysis	Kinematic analysis yields information on the orientation and shape of the stress ellipsoid.
Lateral ramp	Lateral ramps have a strike parallel to the displacement direction, and can be considered tear faults
Leak-off tests	Leak Off Testing is to determine the strength of the rock, commonly also called a pressure integrity test (PIT). During the test, a real-time plot of injected fluid versus fluid pressure is plotted. The initial stable portion of this plot for most wellbores is a straight line, within the limits of the measurements. The leakoff is the point of permanent deflection from that straight portion.
Lithology	The study of the general physical characteristics of rocks.

Local groundwater model	A model of groundwater for a local area.
Matrix (rock matrix)	The finer grained mass of rock material in which larger grains/crystals are embedded
Membrane	A sheet-like structure acting as a boundary or barrier.
Membrane seal	Synonymous with Capillary Seal: A rock layer with sufficiently low permeability as to provide a capillary barrier to the upwards migration of a non-wetting fluid phase.
Methane	The flammable gas (CH ₄), which forms the largest component of natural gas
Milli Darcy (mD)	Measurement unit for permeability
Mohr - Coulomb failure envelope	The linear envelope that is obtained from a plot of the shear strength of a material versus the applied normal stress.
Molecular diffusion	The process whereby solutes are transported at the microscopic level due to variations in the solute concentrations within the fluid phases.
Multi-phase flow	The concurrent flux of more than one fluid phase (e.g. methane and water) through a porous media.
Nested model	A finely discretised detailed numerical simulation set within a coarser discretised regional numerical simulation.
Non-Aqueous-Phase-Liquids	A liquid that is not miscible in formation water
Non-wetting phase	A phase (water or hydrocarbon or other gas) that in combination with a mineral surface has a contact angle of greater than 90 degrees.
Normal stress	The stress which acts perpendicularly to the plane to which a force has been applied.
Numerical groundwater model	A numerical groundwater model divides space and/or time into discrete pieces. Features of the governing equations and boundary conditions (e.g. aquifer geometry, hydrogeological properties, pumping rates or sources of solute) can be specified as varying over space and time. This enables more complex, and potentially more realistic, representation of a groundwater system than could be achieved with an analytical model. Numerical models are usually solved by a computer and are usually more computationally demanding than analytical models.
Permeability	The measure of the ability of a rock, soil or sediment to yield or transmit a fluid. The magnitude of permeability depends largely on the porosity and the interconnectivity of pores and spaces in the ground.
Petroliferous basin	A sedimentary basin that contains hydrocarbons.
Porosity	The proportion of the volume of rock consisting of pores, usually expressed as a percentage of the total rock or soil mass.
Power-law distribution	A straight line correlation on a log-normal graph.
Protolith	A protolith is the original, unmetamorphosed rock from which a given metamorphic rock is formed.
Reactivation potential	The likelihood that a fault will experience a seismic event at a given stress condition.
Recharge	Groundwater recharge is the process whereby surface water (such as from rainfall runoff) percolates through the ground to the water table
Regional groundwater model	A model of groundwater for a regional area.
Relative permeability	A ratio of the total permeability attributable to the wetting and non-wetting phases at a given saturation.
Relay ramp	A type of displacement transfer structure between overlapping normal fault segments.
Reservoir	A stratigraphic layer that has accumulated hydrocarbons.

Rheology	The science of deformation and flow of matter including solids, like rocks.
Seal capacity / potential	The ability of a low permeability geological feature (top or fault seal) to accumulate and retain hydrocarbons.
Seismic	Relating to earthquakes or other vibrations of the earth and its crust.
Seismic lines/data and interpretation	Seismic Interpretation is the extraction of subsurface geologic information from seismic data. The seismic wavelet starts as the pulse of seismic energy generated by an energy source, it travels down through the earth, is reflected and travels back up to the surface receivers carrying the geological information with it. Seismic data is recorded into what is termed the <i>time-domain</i> . Several common processing routines transform the data into a new domain (such as depth), perform various operation and then the inverse routine is used to reverse the transform.
Shale content	The volume of shale or clay minerals per volume of rock.
Shear stress	Shear stress is the stress component parallel to a given surface, such as a fault plane, that results from forces applied parallel to the surface.
Siliciclastic strata	Strata relating to or denoting clastic rocks consisting largely of silica or silicates.
SO ₄	Sulphate
Solute	The substance present in a solution in the smaller amount. For convenience, water is generally considered the solvent even in concentrated solutions with water molecules in the minority
Springs	A spring is a water resource formed when the side of a hill, a valley bottom or other excavation intersects a flowing body of groundwater at or below the local water table, below which the subsurface material is saturated with water. It represents groundwater discharge to surface.
Stratigraphic analysis	The analysis of geological strata.
Strike-slip	A fault in which rock strata are displaced mainly in a horizontal direction, parallel to the line of the fault.
Sub-seismic strain	Deformation or strain occurring at a scale too small to be discerned by seismic analysis.
Tensile stress	A normal stress (negative compressive stress) which pulls apart the material on either side of a plane. Tensile stress greatly weakens rocks, reducing the amount of shear stress that is needed to produce failure in them.
Top-seal	A stratigraphic horizon with sufficiently low permeability to accumulate and retain hydrocarbons.
Unconventional gas	Unconventional gas does not rely on buoyancy and trap geometry as the primary trapping mechanism. Rather, low permeability strata hold gas in place via capillarity or adsorption. In these cases the gas occurs as a continuous phase over large areas independent of trap geometry.
Validation	To prove that something is based on truth or fact.
Wettability	Wettability refers to the interaction between fluid and solid phases. In a reservoir rock the liquid phase can be water or oil or gas, and the solid phase is the rock mineral assemblage. Wettability is defined by the contact angle between two fluids with the solid phase.
Wetting phase	A phase (water or hydrocarbon or other gas) that in combination with a mineral surface has a contact angle of less than 90 degrees.

1 Introduction

The hydraulic influence of faults on groundwater flow has long been recognized by humans because faults often provide a focus of groundwater discharge in the form of springs. Yet the representation of faults and their hydraulic properties are rarely included in regional groundwater models.

There is an extensive body of scientific literature on fault characteristics and their genesis in structural geology journals, however, the understanding of fault hydraulic properties and their transmission (or not) of fluids in sedimentary sequences primarily comes from two domains of research: 1) conventional oil and gas exploration and production geology where faults can either allow hydrocarbons to accumulate in commercial volumes, or to leak rendering an otherwise valid trap to be “dry” or sub-economic, and 2) hydrogeological and ecological research on groundwater springs occurring along faults that come to surface. The economic imperative of having pre drill-predictive capability in estimating fault seal capacity to conventional hydrocarbon accumulations has led to the development of several procedures and techniques that evaluate various aspects of fault zone hydraulic characteristics at various in-situ environmental conditions (pressure, temperature, stress, wettability). These include: fault zone architecture and juxtaposition analysis, mechanical seal capacity and fault reactivation potential, capillary fault seal capacity and hydrodynamic analysis, and sub-seismic strain analysis. The oil and gas industry uses field production histories and observed field compartmentalisation to calibrate and validate methodologies for predicting fault seal capacity and the representative hydraulic parameters of fault zones. In the domain of groundwater hydrogeology, surface water hydrology and ecology, observations of groundwater spring temperature, flux and geochemical characteristics for springs occurring along faults are used to infer fault zone hydraulic properties.

Concerns of aquifer pressure depletion, fugitive methane migration and degradation of aquifer water quality due to CSG development effects propagating up faults can be investigated through the use of regional groundwater models if they are appropriately parameterised. This literature review highlights established methodologies of fault zone characterisation that can be adopted and adapted into a workflow for accurately representing fault zone hydraulic properties in regional groundwater models.

2 Context

The overall project “*Research to improve treatment of faults and aquitards in Australian regional groundwater models to improve assessment of impacts of CSG extraction*” focuses on identifying and assessing technical uncertainty associated with deep groundwater extraction and depressurisation. Recent research, discussions with the Independent Expert Scientific Committee on coal seam gas and large coal mines (IESC) and consultation with industry stakeholders identified the need for a project to specifically address the following three issues:

1. **Aquitards:** Improving understanding of vertical hydraulic conductivity in aquitards to examine the nature of depressurisation at a range of scales.
2. **Faults:** Improving methods and processes for assessing fault properties (including sub-seismic) in coal seam gas (CSG) reservoirs and their impact on production performance. Improving understanding of faults at various scales and their influence on propagating depressurisation to linked aquifers and surface environments. In addition, how do fault properties in the CSG reservoir and adjacent strata impact the nature of pressure propagation to adjacent aquifers or even surface environments?
3. **Modelling:** Improved conceptualisation, representation and parameterisation of aquitards and faults in regional groundwater models to improve quantification of predictive uncertainty in regional groundwater flow and pressure simulation.

This report forms the literature and methodology review of part 2 on Faults. For the faults component, the project aims to:

- Develop conceptual representations of different groundwater flow conditions associated with faults in sedimentary basins, including their influence on connectivity within individual formations, between formations, and between groundwater and surface water environments;
- Demonstrate new methods for generating fault architecture and frequency in regional scale reservoir-type models;

- Demonstrate new methods for characterizing hydraulic behaviour of fault zones and their representation in reservoir-type models;
- Predict hydraulic behaviour of fault and fracture systems in reservoir-type models incorporating stress field analysis and effect of stress changes on fault hydraulic behaviour;
- Undertake numerical simulations and upscaling of the high-resolution fault and fracture systems architecture and hydraulic behaviour into a cellular groundwater flow model.

There are two categories of potential impact to groundwater resources via faults from CSG development that we consider: 1) aquifer pressure depletion, and 2) increased methane either dissolved in groundwater or as a free phase. The physical drivers for these potential impacts are forces derived from variations in pressure, buoyancy (density), wettability (capillarity) or concentration; the rate of transmission is dependent on the transient distribution of rock and fluid properties. The magnitude of any one of these driving forces necessarily increases with proximity to the produced CSG reservoir along the transmission vector.

The nature of fault transmission pathways is investigated in this literature review and summary. In order to improve our ability to represent faults in regional groundwater flow models we must first understand the physical characteristics of faults in different geological settings and the data required to characterise them. We then link this with the various fluid properties (water and its constituents, hydrocarbons and non-hydrocarbon gas) and the transient processes important in governing the movement of various fluids within the faulted rock framework. With this theoretical understanding of faults and fluids established with the best current knowledge, we can then a) examine case studies with example data sets having an eye to understanding the utilisation of data and field observations to validate and calibrate the conceptual fault models; and b) contemplate which methodologies and procedures are most appropriate for incorporating fault zone characteristics into predictive regional groundwater flow simulators.

The literature review conducted here recognises that the majority of research on predicting fault seal characteristics comes from the conventional oil and gas domain. It should also be noted that there is an even larger historical body of work related to structural geology upon which most fault seal analysis research is based. Finally, there is a body of work related to the characterisation of groundwater springs and how these may relate to discharge up faults. In the conventional oil and gas domain the primary objective is to understand and predict fault seal capacity to hydrocarbons in advance of drilling. However to do this, relies fundamentally on predicting fault rock properties such as permeability. We can use the same approaches for predicting fault rock permeability but then apply this knowledge to characterising the degree of compartmentalisation or connectedness of aquifer systems with coal seam gas strata. This knowledge will aid in realistic parameterisation of regional groundwater flow models.

3 Assumptions and Methodology

In this review we assume that the primary intent is to try and more accurately estimate the hydraulic properties and characteristics of faults and that we need to do this for a multiphase system that contains both formation water and hydrocarbons.

In order to assess the hydraulic properties of faults it is important to first consider the time-scale in question and which type of data apply to each time-scale. These could be:

- Geological time-scale where we use data that has not been affected by production of water or hydrocarbons; and
- Human time-scale where we are interested in fault seal performance over periods of years to tens of years.

In order to gain an understanding of the fault systems we take the approach of first examining data (pre-Production) that can provide information/evidence on the hydraulic properties of faults at the geological time scale. With this characterisation, we can then consider how these hydraulic properties will manifest in human time-scale fault seal performance and if the rock properties themselves are transiently affected by anthropogenic changes of formation pressure. In the situation where formation pressure may be changing over time, this results in changes to the effective stress in the sub-surface and a change in effective stress can result in a change in permeability. To understand fluid flow in regional groundwater models in a situation

where both in-situ stress and permeability are transient, it may require a dynamic permeability update at certain time steps of the groundwater flow model.

To gain an understanding of fault hydraulic properties there are two main sets of observations that provide direct evidence: 1) observations of hydrocarbon interactions with faults at geological time-scales, and 2) observations of springs that discharge to surface along faults at human time scales. We therefore have a strong focus of utilising these systems to define our analytical methodologies. The rock properties that we can estimate with these methodologies can then also be applied to faults within formation water flow systems represented by regional groundwater models.

4 Definitions and Terminology

This report is aimed at understanding techniques and methodologies that can be used, adapted or developed to improve the characterisation of faults and their inclusion in regional groundwater models. Much of the previous work on prediction of fault properties comes from the petroleum engineering or oil and gas exploration literature. Groundwater resources professionals often use terminology that is equivalent but different from engineers and geologists working in the oil and gas industry. As such, it is worth-while to clarify some terminology that will be used in this report.

Reservoir vs Aquifer: Hydrogeologists use the generic term “Aquifer” to refer to a stratigraphic rock unit having hydraulic properties such that useable groundwater volumes can be produced. This is roughly equivalent to the generic term “Conventional Reservoir” used by oil and gas professionals where the reservoir rock has hydraulic properties from which oil or gas can be economically extracted. Both reservoir and aquifer terminology can have modifier descriptors that indicate a range of characteristics such as “good aquifer” or “poor aquifer” or “excellent reservoir” or “marginal reservoir”.

Seal vs Aquitard: Hydrogeologists use the generic term “Aquitard” to refer to a stratigraphic unit having hydraulic properties such that no appreciable groundwater can be produced but which allows formation water leakage over longer time-scales. This is roughly equivalent to the generic term “Seal” used by oil and gas professionals where the seal rock has hydraulic properties which trap or prevent the migration of oil or gas. Both aquitard and seal terminology can have modifier descriptors that indicate a range of characteristics such as “strong aquitard” or “weak aquitard” or “tight seal” or “leaky seal”. Additionally, hydrogeologists often refer to an “Aquiclude” as a stratigraphic unit with such low permeability that no leakage of formation water can occur across it. Given long enough observational time-scales very few strata can be considered aquicludes by the strict definition however strata such as evaporite horizons may qualify.

Multi-Phase Flow vs NAPL or DNAPL: Contaminant hydrogeologists often deal with Non-Aqueous-Phase-Liquids (NAPL’s) or Dense-Non-Aqueous-Phase-Liquids (DNAPL’s) where fluid viscosity and surface tension are important to understand capillary forces. The equivalent for Oil and Gas industry professionals is multi-phase flow where the wettability (contact angle between the formation water, the hydrocarbon and the mineral surface) of the oil or gas phase relative to formation water and the surface tension is related to capillarity. This is often expressed as a “relative permeability” where the permeability of a particular rock differs depending on the characteristics and physical properties of the fluid in question.

Formation Pressure vs Water Level: Hydrogeologists dealing with water bores often have physical access to the well-head and can measure the standing water level in a bore. This value can be corrected for density effects and converted to a hydraulic head representative of the aquifer at the screened interval. Oil and Gas wells have multiple levels of well control to make them safe in the presence of (or potential for the presence of) buoyant and flammable hydrocarbon phases. For oil and gas wells the formation pressure is measured by downhole devices such as Drill Stem Tests (DST’s), Wireline Tests (WLT’s such as Modular Dynamic Tests (MDT’s) or Repeat Formation Tests (RFT’s)), and production tests or from pressure kicks recorded during drilling. These types of pressure tests are often conducted as part of a temporary well completion where a flow and pressure build-up is collected over multiple cycles. The pressure-time data often requires extrapolation in a Horner type analysis to estimate the in-situ formation pressure. The extrapolated formation pressure can be subsequently converted to hydraulic head to understand the fluid potential of the aquifer at the completed interval. These type of tests also often provide a fluid sample that can be analysed in the laboratory.

Membrane Seal vs Capillary Seal: These two terms are used interchangeably in the fault seal analysis literature but for simplicity we use capillary terminology in this report. All aspects of capillarity are explained in relation to fault seal and multi-phase flow within the text to follow.

Water Bore or Monitoring Bore vs Oil or Gas Well: The groundwater industry normally refers to “bores” and the oil and gas industry refers to “wells”. Whilst basically the same concept they tend to have very different design. Water bores may or may not be cased, they may or may not have a well head that can control pressure, and they more than likely have a filter pack and screened interval that allows formation water to enter the bore without the bore clogging. Oil and gas wells are designed to provide multiple barriers between the hydrocarbon and formation water aquifers. These often include multiple casings and well head features to control well head pressure.

Fault Reactivation: Refers to the mechanical strength of a fault being overcome by changes in pore pressure that alter the effective stress. The term “induced seismicity” refers to the seismic energy (earth quake) that results from an anthropogenic fault reactivation event.

5 Fault Zone Physical Characteristics

An overarching goal of fault zone analysis is to accurately estimate fault zone hydraulic properties that may influence the hydraulic connectivity either across a fault at a single elevation (i.e. in a direction perpendicular to the fault plane surface) or along or up a fault plane between aquifers (i.e. within the fault plane surface). *Fault seal capacity* is the term used to describe the capacity of the fault to impede the flux of one or more fluid types. State of the art fault seal capacity analysis requires an evaluation of the stratigraphic heterogeneity of the broader host rock (on either side of the fault), linked with associated rock and fluid properties. Uncertainty in these parameters directly impacts the accuracy of determining fault rock properties. Fault zones may either compartmentalise strata horizontally, cause localised vertical hydraulic connectivity between stratigraphic levels or both. There are several aspects of fault zones that can either allow for this hydraulic communication or prevent it. These require different assessment methods, which generally rely on similar underpinning data sets. Integration of these analytical processes, supported by hydrodynamic and hydrochemistry data is required to assess the fault seal capacity and assign fault zone hydraulic properties to groundwater models.

In many petroliferous basins, fault seal effectiveness has proven to be a significant uncertainty affecting exploration success, and this translates to uncertainty in predicting reservoir and seal performance within the oil and gas industry. Faults can be leaky simply by virtue of the detailed fault zone architecture within the prevailing stress regime, or fault seals can be breached by capillary leakage or fault reactivation. Various authors have classified seals according to the sealing mechanism (e.g. Watts 1987; Heum 1996; Bretan *et al.* 2003; Brown 2003).

Faults can provide capillary seal capacity either through juxtaposition of reservoir against a seal, or by the low permeability of the gouge and cataclastic material in the fault zone itself (Watts 1987). When the fault capillary seal capacity is exceeded, leakage of hydrocarbons can occur across or along the fault depending on the fault zone architecture. If the formation pressure exceeds the mechanical strength of the fault rock then the seal may fail due to fault reactivation. To help standardise the nomenclature for various aspects of hydrogeology and capillary seal terminology discussed in this report, a table of symbols and a glossary is provided at the start of this report.

5.1 Fault Zone Architecture and in-Situ Stress

Faults can be classified according to their geometry and relative sense of movement into a) normal, b) reverse, c) strike-slip, and d) oblique, coupled with various amounts of rotation of scissor relative movement (Figure 1). Uncertainty regarding seal leakage can be reduced by analysing key leak risk points on fault systems (e.g. Gartrell *et al.* 2002 and Gartrell *et al.* 2006). These often occur at the intersection of high angle steeply dipping faults (Craw 2000) or at relay ramps (Underschultz *et al.* 2003) as shown in Figure 2 and Figure 3, where the continuity of the fault plane is interrupted (Gartrell *et al.*, 2004; Cowley and O’Brien, 2000) and there is structural complexity. It is also at these locations where fault segments often have an orientation relative to the stress field that results in dilatant conditions. Fault or fracture orientation relative to the stress field can be characterised in terms of “Dilatancy Potential” which may in turn be associated with a permeability estimate. These higher permeability zones or leak points have characteristic signatures, often identifiable with hydrodynamic analysis (Underschultz *et al.* 2005), where they form anomalies in the pressure, water chemistry

and/or temperature distributions. The following analysis method can be used, drawing on fault zone architecture and in-situ stress:

- Geometric analysis of kinematically realistic fault interpretations within a three-dimensional anisotropic stress field. This determines the locations along the fault zone and on various fault segments where the fault geometry is in tension, compression or shear. Within this context, the dilatant tendency of the fault and associated damage zone can be determined, which affects hydraulic transmissivity. This work can be conducted in the first instance simply by using the fault plane statistics from the seismic interpretation and the in-situ stress analysis. A more rigorous analysis could be conducted using software such as FaultRisk (<https://www.faultseal.com/>), FAST (Mildren & Hillis, 2002) or TrapTester¹; and
- Fault and fracture orientation and intensity may be inferred to some extent by analysis of the data from seismic lines. Walsh and Watterson (1988) and Gillespie et al. (1993) identified a fractal relationship between fracture populations at different scales, which has been shown to be valid for sub-populations at different azimuths. This suggests that a careful quantitative analysis of the observable faults can lead to a prediction of the population of smaller faults at different orientations (see Section 5.3).

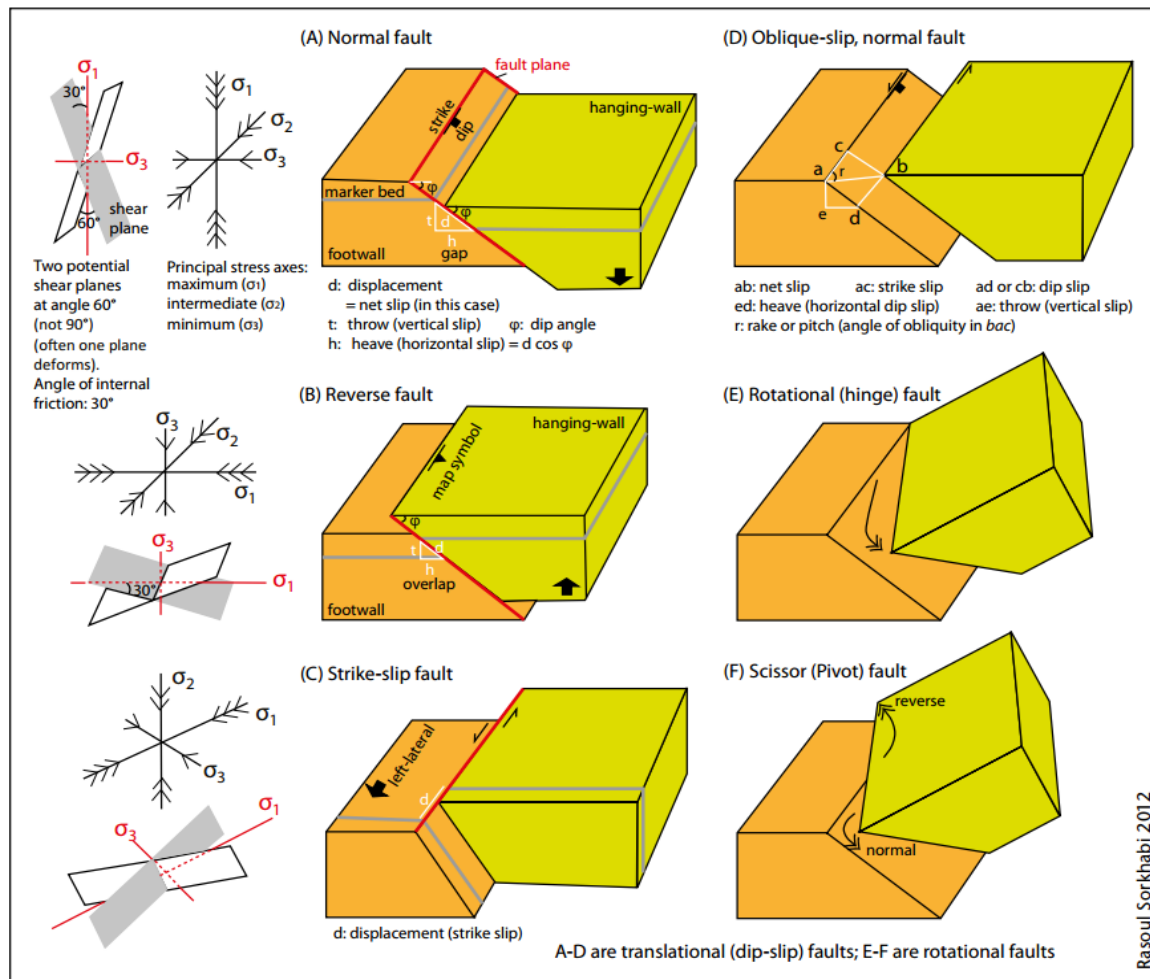


FIGURE 1. FAULT STYLE SKETCHES SHOWING THE PRINCIPAL STRESS AXES AND SLIP CLASSIFICATIONS OF VARIOUS FAULTS. NOTE THAT IN THEORY ALL FAULTS HAVE A CERTAIN AMOUNT OF ROTATIONAL COMPONENT BECAUSE DISPLACEMENT, EVEN IN A DIP-SLIP FAULT, VARIES ALONG THE FAULT LENGTH. HOWEVER, IN A ROTATIONAL FAULT THE VARIATION IS GREATER BETWEEN TWO NEARBY POINTS ALONG THE FAULT STRIKE THAN CAN BE ACCOUNTED FOR SIMPLY BY THE FAULT PLANE GEOMETRY. (SORKHABI, 2013).

¹ <http://www.badleys.co.uk/traptester-overview.php>

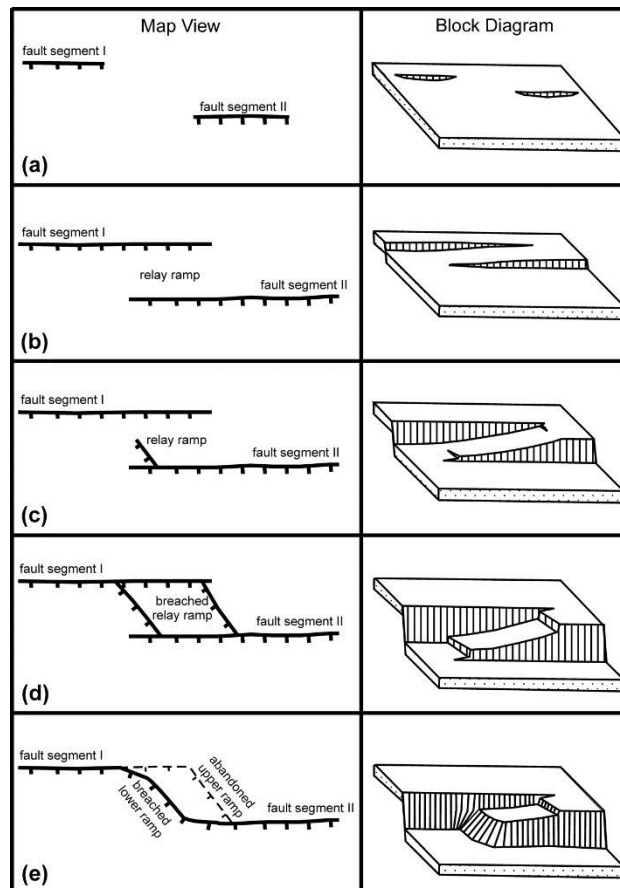


FIGURE 2. SCHEMATIC DIAGRAM SHOWING EVOLUTIONARY STAGES OF A RELAY RAMP. TICK MARKS ON THE MAP VIEW DEPICT THE DOWN-THROWN BLOCK OF NORMAL FAULTS. (A) STAGE I: THE FAULTS DO NOT INTERACT. (B) STAGE II: THE FAULTS HAVE STARTED TO INTERACT AND A RELAY RAMP HAS DEVELOPED TO TRANSFER THE DISPLACEMENT AMONG THE SEGMENTS. (C) STAGE III: ACCUMULATED STRAIN IN THE RELAY RAMP HAS RESULTED IN INITIATION OF FRACTURING. (D) STAGE IV: THE RELAY RAMP IS BROKEN BY A BREACHING FAULT TO FORM A SINGLE FAULT ZONE WITH STRIKE IRREGULARITY. (E) UPPER BENCH IS ABANDONED AND TWO SEGMENTS JOINED THROUGH BREACHING OF LOWER RAMP THAT FORM AN ALONG-STRIKE BEND ON THE COURSE OF THE MAIN FAULT. CIFTCI AND BOZKURT (2007) MODIFIED FROM PEACOCK & SANDERSON (1994).



FIGURE 3. A PHOTO OF A RELAY RAMP BETWEEN ~8CM DISPLACEMENT NORMAL FAULT SEGMENTS IN THE LIASSIC LIMESTONES AND SHALES OF KILVE, SOMERSET, UK (FAULT ANALYSIS GROUP, DUBLIN²).

² <https://www.fault-analysis-group.ucd.ie/gallery/relay.htm>

The seismic characterisation should consist of:

- Review of available data and existing interpretations about type, extent, displacement and location of faults;
- Interpretation of seismic line data using well logs and kinematic analysis to constrain correlations of fault intersections between various seismic lines including assessing the fault throw and the fault vertical extent. Use of 3D seismic volumes (where available) can reduce the fault correlation uncertainty;
- Construct a 3D fault model consisting of 3D surfaces representing the interpreted faults;
- Assess the sufficiency of the existing seismic surveys to adequately characterise fracture intensities and to estimate different fault orientations, considering the direction and spacing of seismic lines relative to expected fault orientations; and
- Review the interpreted fault architecture in the context of outcrop analogues.

An example of fault zone architecture can be gained from outcrop analogue studies such as that shown in Figure 4. These can be related back to a subsurface characterisation constructed from seismic interpretation.

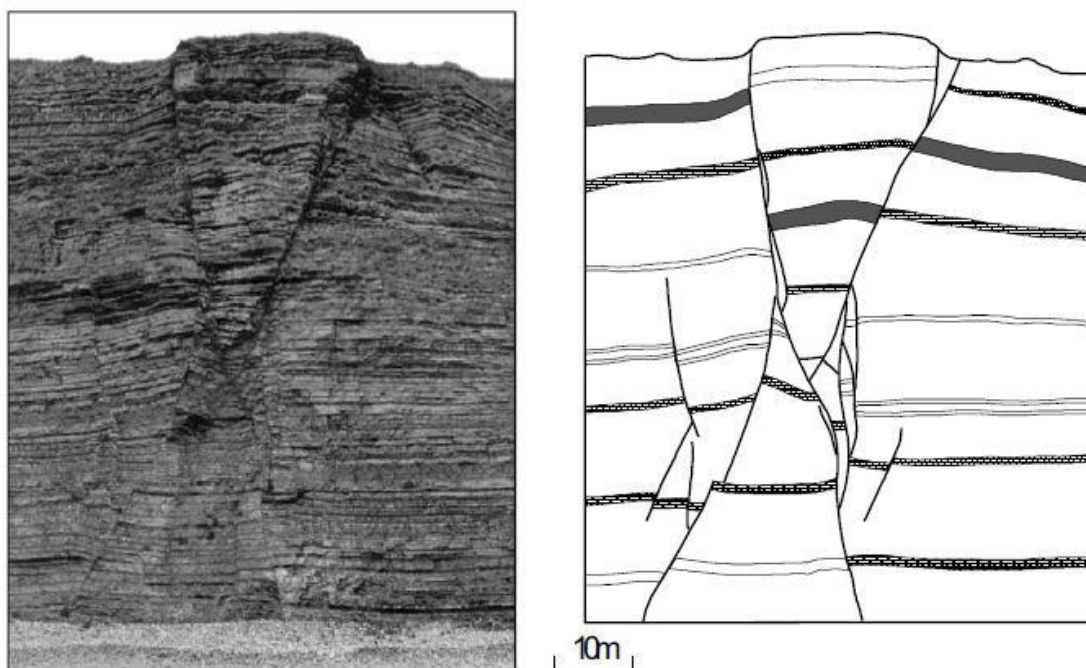


FIGURE 4. CONJUGATE FAULT SYSTEM EXPOSED IN A 60 M HIGH VERTICAL CLIFF SECTION OF LIASSIC LIMESTONE, NASH POINT, SOUTH WALES. FROM WATTERSON ET AL. (1998) AND IMAGES PROVIDED BY FAULT ANALYSIS GROUP, DUBLIN¹.

5.2 Mechanical Seal Capacity of Faults and Fault Reactivation

In the context of this literature review it is important to consider the transient component of the CSG development cycle and how this may relate to changing fault seal capacity over time. Primarily this is the result of the transient induced pressure conditions that occasionally includes a short period of increased pressure during reservoir stimulation but is dominated by progressive pressure decline of the CSG reservoir and the related changes to effective stress. The pressure decline phase could occur over a 30-40 year development plan and then recovery could occur over that much again or longer (CH2MHILL, 2013). To incorporate this in regional groundwater models may require a novel approach of coupling with geomechanical modelling. The end result is that a transient permeability field may require consideration. To accomplish this a coupled modelling process could be designed where at each time step the change in formation pressure (P) could be input to a geomechanical model (e.g. FLAC or COMSOL multiphysics) that updates the permeability distribution based on the new effective stress. This new permeability distribution could in turn be used to update the groundwater flow model for the proceeding time-step. These coupled

approaches have been used at the hydrocarbon field-scale (Zhang et al., 2011) but not to our knowledge in a regional groundwater model.

The reactivation potential can be evaluated by examining the fault zone orientation in combination with the mechanical strength of the fault, the in-situ stress and the pore pressure (Mildren et al. 2002). The areas with the highest chance of reactivation are fault bends orientated at critical angles to the stress field (Gartrell et al., 2002). As the effective stress changes due to a change in pore pressure or overburden load, it will move the fault zone stress condition relative to the failure condition (either closer or further away). The distribution of effective stress relative to the failure criteria under various transient conditions can be used to map relative likelihood of fault reactivation on the fault plane. This can be examined with a Mohr-Coulomb type analysis. Additionally, hydrodynamic techniques can be employed to characterise the pore pressure distribution, and the change in pore pressure over time (Underschultz, 2005).

The mechanical fault reactivation potential analysis should consist of:

- Obtaining in-situ stress and the degree of its anisotropy evaluated from borehole image logs, wireline calliper logs, leak off tests (if available regionally), and other geophysical measurements;
- Obtaining a pore pressure distribution from hydrogeological bores and O&G wells where the formation pressure is estimated on either side of faults across multiple hydrostratigraphic units;
- Rock strength data obtained from laboratory geomechanical and rock physics measurements on core;
- The detailed orientation of the fault zone and its relation to the in-situ stress; and
- Creation of reactivation potential and slip tendency maps using Mohr-Coulomb analysis.

The reactivation potential and slip tendency evaluation for faults can be conducted using software such as the Fault Analysis Software Tool (FAST) developed by the University of Adelaide (Mildren & Hillis, 2002). Results can be used to understand the magnitude of stress change (equivalent to a pore pressure change) that can be accommodated prior to fault reactivation. It can also be used to identify the highest likelihood orientation within a fault population to be reactivated or particular fault segments of higher reactivation potential. This could be used as a guide to monitoring design. An example is shown in Figure 5 (Bailey et al. 2006) where Mohr-Coulomb analysis is conducted for a range of fault segment orientations.

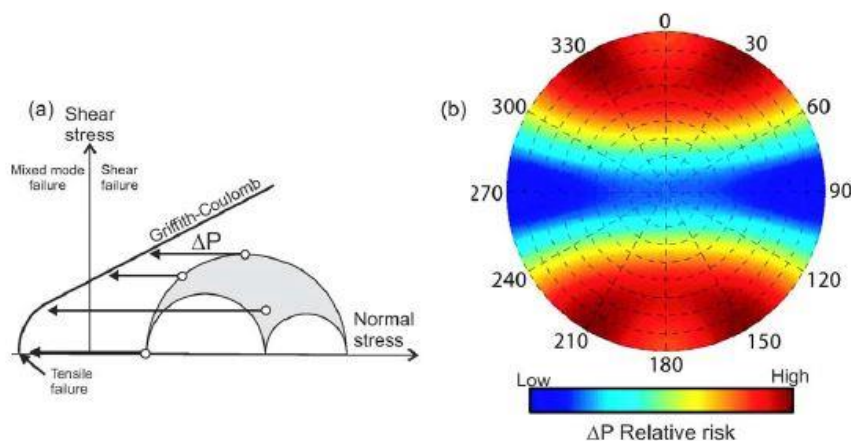


FIGURE 5. (A) GRAPHICAL REPRESENTATION OF THE FAST METHOD FOR RISKING THE LIKELIHOOD OF FAULT REACTIVATION USING A MOHR-COULOMB DIAGRAM (AFTER MILDREN ET AL., 2002). THE SMALLER THE ΔP VALUES (DIFFERENCE BETWEEN EFFECTIVE STRESS AND THE FAILURE CRITERIA), THE HIGHER THE RISK OF REACTIVATION. (B) POLAR PLOT SHOWING THE DISTRIBUTION OF ΔP VALUES FOR POLES TO FAULT PLANES FROM THE PYRENEES-MACEDON OIL AND GAS FIELDS. THE HIGHEST RISK OF REACTIVATION (LOWEST ΔP ; DARK RED) IS ON STEEPLY DIPPING FAULTS STRIKING 060° AND 120°, AND E-W FAULTS DIPPING AT 60° (BAILEY ET AL. 2006).

The reactivation of faults can also be influenced by the overall fault zone architecture. Gartel et al. (2005) examined how strain localisation can be controlled by the distribution of pre-existing large and small faults (Figure 6) based on case studies from the Laminaria High on Australia's North West Shelf. Langhi et al (2009), Zhang et al. (2009), Langhi et al (2010) and Zhang et al. (2011) follow this up with geomechanical modelling for the impact of extension on a rock volume with different geometries of pre-existing fault populations under

various fluid pressure conditions. These were variously fashioned on observed fault populations in the North West Shelf.

Reactivation potential for faults in the context of CSG development may be important over the life of field development. As the reservoir is pressure depleted the effective stress changes and the nature of fault seal capacity could have a transient component that can be built into regional groundwater models.

5.3 Sub-Seismic Strain

Many fault analysis approaches are criticised because they apply only to the observable strain (which can be identified on seismic or other geophysical methods such as gravity or electromagnetics). There is also strain existing that is of a magnitude less than what can be observed by these methods. The sub-seismic strain, as represented by fracturing and minor faulting, can influence seal capacity (ie aquitard permeability) and is important to understand and predict.

Fractures and faults exhibit a strong relationship between maximum displacement (fault throw) and fault length (Figure 7). In addition, for a given volume of rock, the total strain will be taken up by faults and fractures with a range of sizes. This population of faults and fractures often define a power-law throw distribution where there is a higher frequency of small displacement faults and a lower frequency of large displacement faults (e.g. Ackermann et al., 2001, Meyer et al., 2002; Manzocchi et al., 2009). If only a portion of the total fault population can be observed, the remainder of the power law distribution can be extrapolated to predict the unobserved faults' size distribution (Yielding et al., 1996). Note that this does not elucidate the distribution of sub-seismic strain. Dee et al. (2007) have shown that small brittle faults are not reliably imaged by seismic reflection methods when their offset is less than the seismic resolution (~ 20 m in many on-shore seismic datasets).

Geomechanical approaches have also been used to predict the likely distribution of subsurface strain based on the orientation of in-situ stresses and the intensity and nature of observed brittle deformation (Bourne and Willemse 2001; Bourne et al. 2001; Maerten et al. 2002). Dee et al. (2007) demonstrate that the following method is useful in providing a prediction of small-scale faults and fractures distribution.

The fault slip pattern mapped from seismic data is the primary input data. The algorithms of Okada (1992) can be used to compute the displacement vector and fault-related strain tensor at any observation point in the rock volume surrounding a fault. The predicted rock fracturing resulting from the total stress can then be estimated by comparing the state of stress to a standard Mohr–Coulomb failure envelope defined by an appropriate coefficient of internal friction and cohesive strength. The maximum Coulomb shear stress (Jaeger and Cook 1979) can then be used as a proxy for fracture intensity (Maerten et al., 2002).

This approach can be calibrated against fracture identification from borehole image logs. An example of a power law and subsequent geomechanical analysis can be seen in Figure 8 as described by Langhi et al. (2013) for the Perth Basin strata near the proposed SW Hub carbon geosequestration site.

The sub-seismic strain analysis should consist of:

- Power law analysis on observable faults to identify what portion of the total strain is sub-seismic and the likely fracture size distribution (see Figure 8). It can also indicate that larger faults might exist which having yet to be identified in the seismic analysis;
- Geomechanical analysis involving the identification of the most likely geographic distribution of sub-seismic strain; and
- Calibration with well bore image logs: the analysis of sub-seismic strain can be calibrated against observations of small-scale strain identified in image logs (cm to m scale).

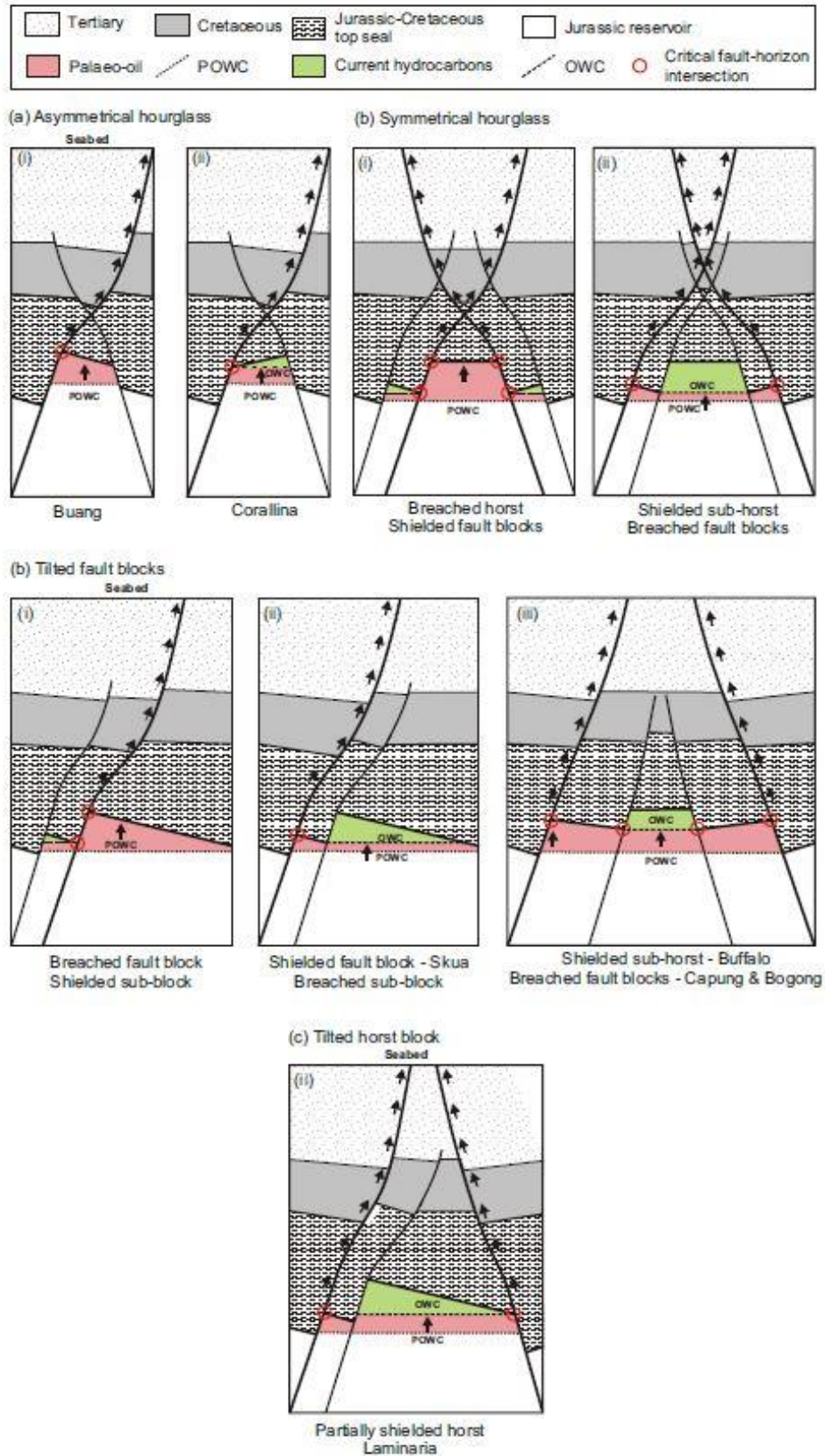


FIGURE 6. SCHEMATIC REPRESENTATION OF TYPICAL FAULT REACTIVATED TRAP GEOMETRIES AND THEIR PREDICTED OIL COLUMN PRESERVATION CHARACTERISTICS. ARROWS DEPICT HYDROCARBON LEAKAGE ALONG HIGH STRAIN FAULTS ABOVE THE CRITICAL FAULT-HORIZON INTERSECTIONS. NOTE HOW CERTAIN FAULTS ARE "SHELTERED" BY REACTIVATION OF OTHER NEARBY FAULTS (GARTELL ET AL. 2005).

The sub-seismic strain analysis can provide assurance that the entire range of strain has been considered and data included in the seal capacity analysis. These estimates of sub-seismic strain and their most likely hydraulic characteristics can be taken into account in regional groundwater models either by the same stochastic or upscaling approaches that are applied to the observed strain, or in a staged approach. It could be that up to a certain scale of brittle deformation, fractures and small faults (that make up the damage zone of larger faults) are best up-scaled to an effective K (either into an equivalent single porous medium or a dual permeability rock depending on the distribution characteristics of the strain) using stochastic approaches. Above a certain brittle deformation scale, the strain may be better dealt with as discrete fault/fracture models. These up-scaling strategies will be explored in the Modelling component of the project.

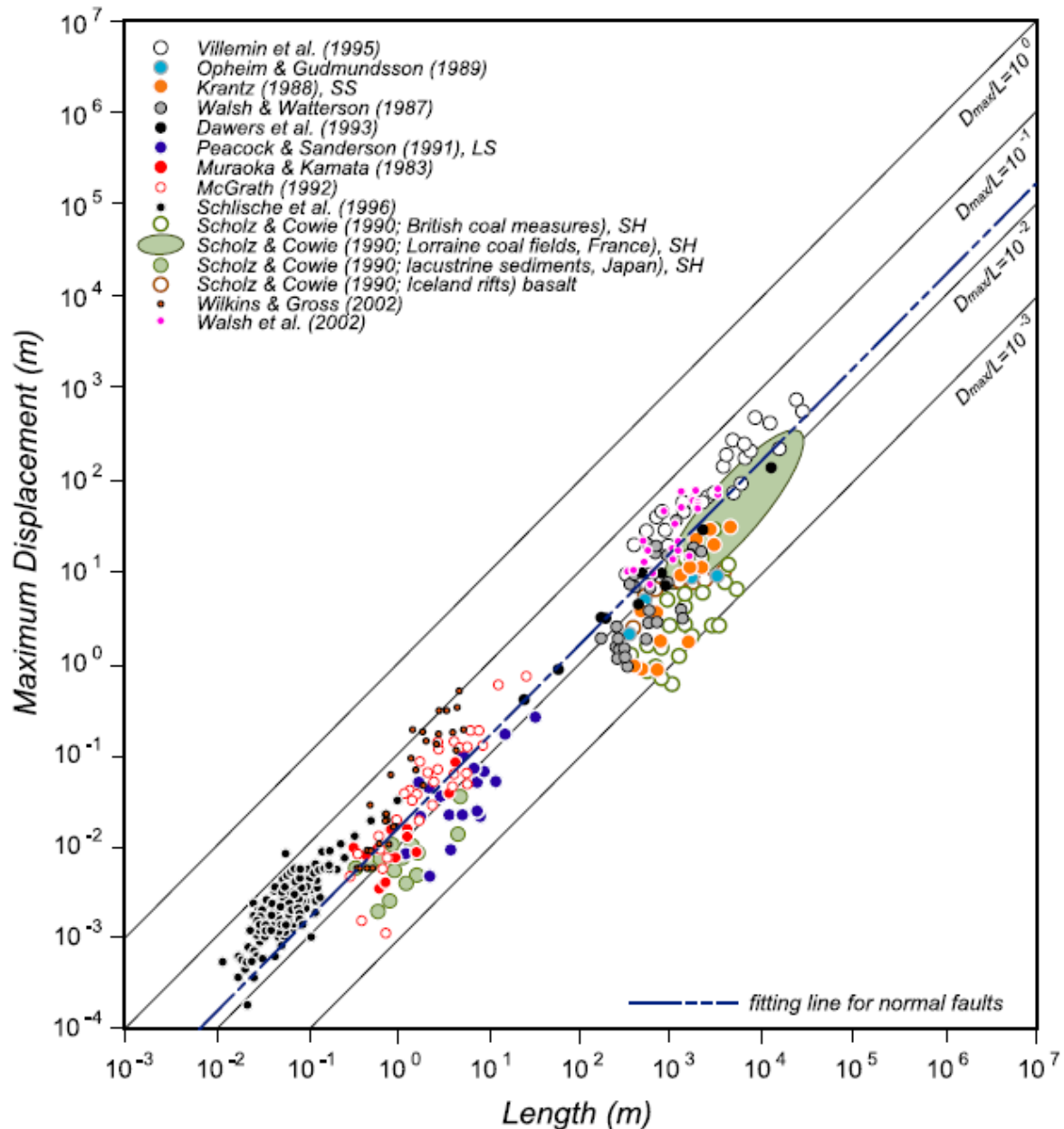


FIGURE 7. PLOT OF MULTIPLE GLOBAL DATA SETS SHOWING MAXIMUM DISPLACEMENT (D_{max}) AGAINST FAULT LENGTH (L) FOR NORMAL FAULTS (KIM & SANDERSON, 2005).

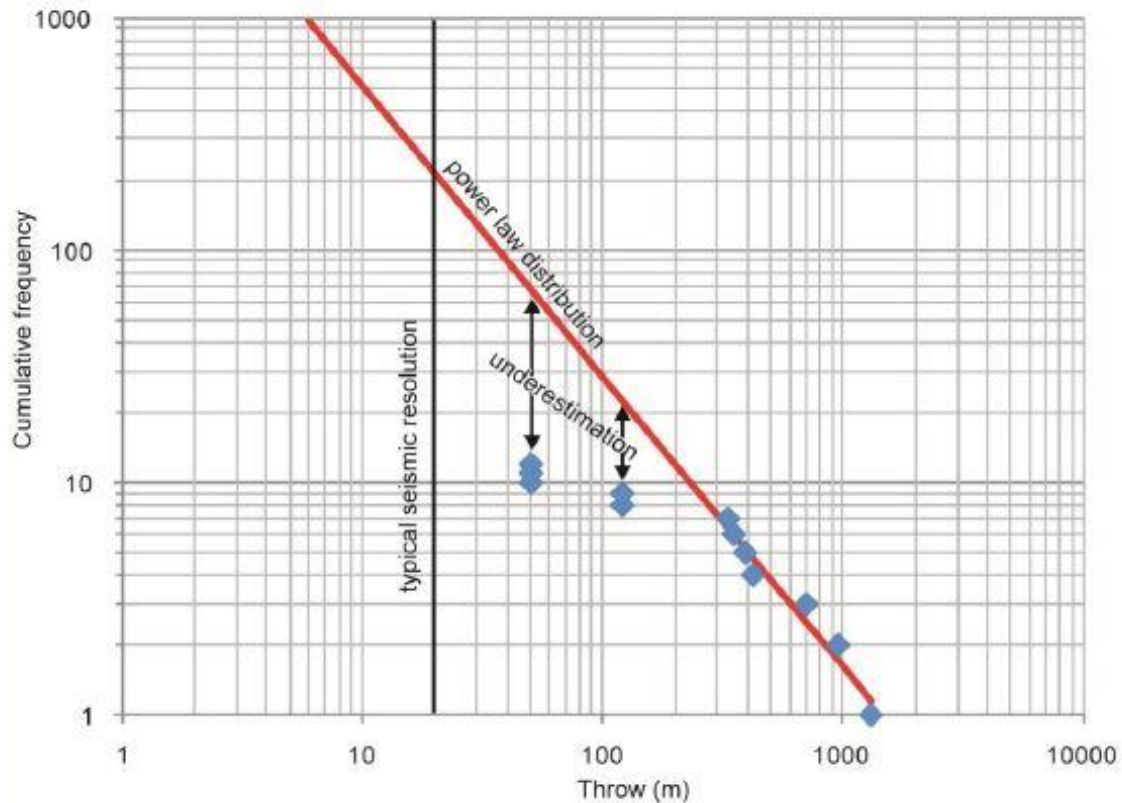


FIGURE 8. POWER LAW DISTRIBUTION OF FAULT POPULATION THROWS AT THE SW HUB PROPOSED CARBON STORAGE SITE IN WESTERN AUSTRALIA: PERTH BASIN (LANGHI ET AL. 2013).

5.4 Permeability of Faults, Across Fault Leakage and Capillarity

For the purposes of this literature review, capillary related processes become important when considering the movement of hydrocarbons (mainly methane) across seals in the subsurface. Unless dealing with organic rich low permeability strata (Iglauer et al. 2015), we assume the hydrocarbon is the non-wetting phase and water the wetting phase. This is normally appropriate for fault rock. In this wettability situation, any time a migrating hydrocarbon encounters a change in permeability to a lower value there will be additional capillary forces that need to be overcome prior to the hydrocarbon continuing to migrate. This is an important factor to consider if regional groundwater models are used to predict fugitive methane migrating into shallow aquifers or to the surface as seeps or in spring discharge. Note that capillary barriers occur only when moving from higher to lower permeability along a migration pathway for the non-wetting phase. Current research on wettability, relative permeability and implications for multiphase flow include Iglauer et al. (2015), Heller et al. (2014), Pini and Benson (2015), Krause and Benson (2015), Apourvari and Arns (2016) and Herring et al. (2015).

A change in permeability that presents a capillary barrier can occur due to a fault providing juxtaposition of various lithologies (see Figure 9). Alternatively, the permeability of the fault material itself may be lower than the host rock. In recent years there have been several published methodologies for estimating fault-derived permeability indicators. Several not entirely independent precursors to Shale Gouge Ratio (SGR) have been proposed such as CSP (Clay Smear Potential, Bouvier et al. 1989, Fulljames et al. 1997) and SSF (Shale Smear factor, Lindsay et al. 1993). SGR however, has become a commonly used approach (Yielding et al. 1997, Manzocchi et al. 2009, Yielding 2002, Bretan *et al.* 2003), largely due to the robustness of the algorithm which estimates a SGR using commonly available well data such as a V_{shale} log (where V_{shale} represents the % of clay relative to sand or silt in a particular interval thickness). For convenience, this report considers capillary seal capacity in the context of SGR, however, all of the methodologies and conclusions can equally be applied to other fault-derived permeability indicators. Even if capillary forces are not an important consideration, the approaches described here still provide methodologies for assessing fault zone permeability useful in parameterising fault properties in regional groundwater models.

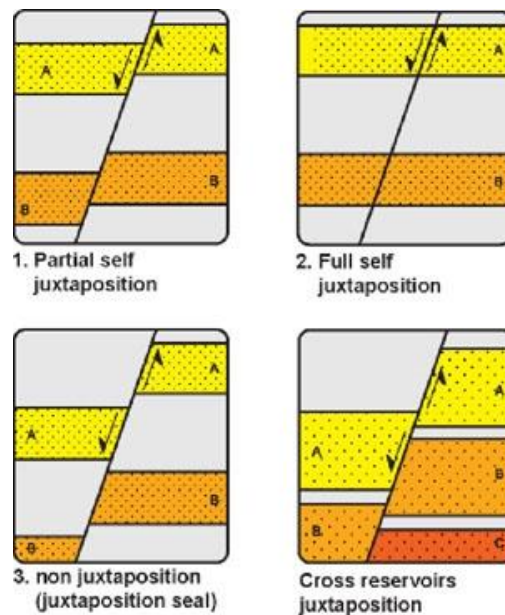


FIGURE 9. SCHEMATIC DIAGRAM OF VARIOUS JUXTAPOSITION ORIENTATIONS (NEELE ET AL. 2012).

5.4.1 Juxtaposition

Juxtaposition diagrams (or “Allan Diagrams”) form a staple of fault seal analysis (Allan, 1989). These diagrams utilise information of the stratigraphy either side of a particular fault plane segment (e.g. Bailey et al. 2006). If the facies distributions and associated rock properties are known, a geometrical analysis will create a map of the fault surfaces that show which rock types are juxtaposed across the fault (e.g. sand on sand, sand on shale, shale on mud, mud on mud etc.). The nature of the rock type juxtaposition provides an estimate of the across fault leakage potential based simply from the rock properties of the host rock. Here for example, the cross sectional areas of sand on sand contacts provide an opportunity for across fault hydraulic continuity.

Case studies such as Bailey et al. (2006) show that juxtaposition alone often does not adequately describe the seal potential of a fault. Hydrodynamic and hydrochemical analysis in faulted strata (Underschultz et al. 2005, and Underschultz et al. 2003) can be combined with juxtaposition diagrams and this can help to determine if additional fault seal analysis is required for adequate assessment of seal capacity. It should be noted that the stratigraphic analysis and a detailed characterisation of the internal distribution of rock types and rock properties is crucial to creation of a well constrained juxtaposition analysis.

The juxtaposition analysis should consist of:

- Using the outputs of the stratigraphic and fault architecture modelling in the form of a 3D static model.
- Development of Allan Diagrams for individual mapped fault surfaces using software such as Petrel³, FaultRisk⁴, or TrapTester⁵.

The outcomes will be Allan Diagrams (Figure 11) showing where sand on sand, shale on shale, or sand on shale contacts occur across each fault plane segment; and an assessment of the distribution of across fault hydraulic communication or isolation on each fault segment. The next step for groundwater modelling is to account for this across fault geometry and the implications for fault transmissivity. Note that the throw distribution on faults is often represented as a rotation rather than a planar movement and this results in particular geometric shapes for juxtaposition domains on a fault plane surface.

³ <http://www.software.slb.com/products/platform/Pages/petrel.aspx>

⁴ <https://www.faultseal.com/>

⁵ <http://www.badleys.co.uk/traptester-overview.php>

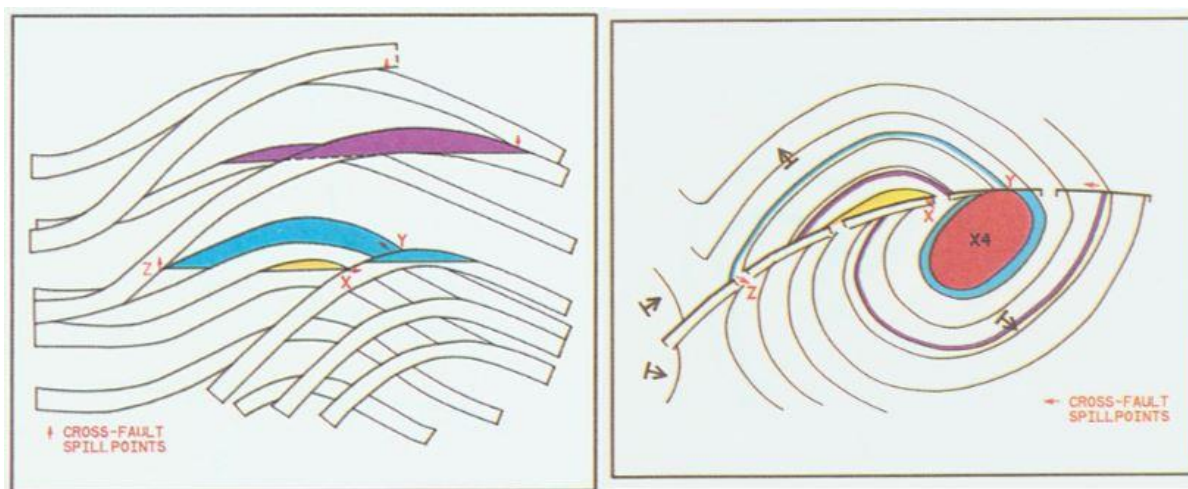


FIGURE 10. AN EXAMPLE OF AN ALLAN DIAGRAM (LEFT) THAT SHOWS ACROSS FAULT JUXTAPOSITION OF MULTIPLE STACKED AND FOLDED SANDSTONE RESERVOIR LAYERS. THE RESULTING ACROSS FAULT HYDRAULIC COMMUNICATION CONTROLS THE HYDROCARBON SPILL POINTS AND HYDROCARBON COLUMN HEIGHTS. THE PLAN VIEW OF THE SAME STRUCTURE (RIGHT) SHOWS THE TRAP GEOMETRY RELATIVE TO THE FAULT TRACE (ALLAN, 1989).

5.4.2 Shale Gouge Ratio (SGR)

FOR ANY GIVEN POINT ON A FAULT SURFACE, **SGR** IS EQUAL TO THE NET SHALE CONTENT OF A GIVEN ROCK THICKNESS WHICH HAS MOVED PAST THAT POINT. **SHALE GOUGE RATIO** CALCULATIONS CAN BE CONDUCTED, AS SHOWN IN

Figure 11, according to Yielding et al. (1997), and these can be related to fault zone permeability (Sperrevik et al. 2002 and Gibson, 1998). The standard approach for calculating across fault pressure difference is to use the pressure profile on either side of the fault as described by Underschultz (2007). Bense (2004) demonstrated how fault zone parameterisation such as SGR had application in understanding fault zone hydraulic properties even at shallow depths where faults come to the surface. Capillary seal capacity can be estimated with the following inputs:

- Stratigraphic heterogeneity characterisation: the different sedimentary facies within the strata on either side of a fault are important to know for SGR calculation as these relate to the volume of shale on either side of a fault. There is a correlation between this and the amount of shale gouge at any location on the fault plane as a function of throw (Yielding et al., 1997).
- Fault zone architecture: the geometry of the fault zone and the orientation of the various fault segments forms a key input to understanding the SGR. The distribution of throw on the fault plane needs to be mapped and this forms an input parameter to the SGR calculation.
- Shale Gouge Ratio mapped on the fault plane: The SGR distribution on the fault plane will be calculated as a function of the shale volume distribution and the throw distribution.
- Pore pressure distribution (from groundwater bores or oil and gas wells): the detailed pore pressure in the strata on either side of the fault forms the important calibration parameter of across fault pressure difference. This distribution will be mapped and plotted against SGR in order to obtain a permeability estimate for given SGR values.
- Map the across fault pressure difference sustainable prior to capillary seal failure and estimate the fault zone permeability distribution.

Development of SGR data for individual mapped fault surfaces will be done using software such as Petrel¹, FaultRisk², or TrapTester³. The data obtained from the SGR analysis leads to an estimate of the fault zone permeability distribution that can directly be utilised in populating regional groundwater models.

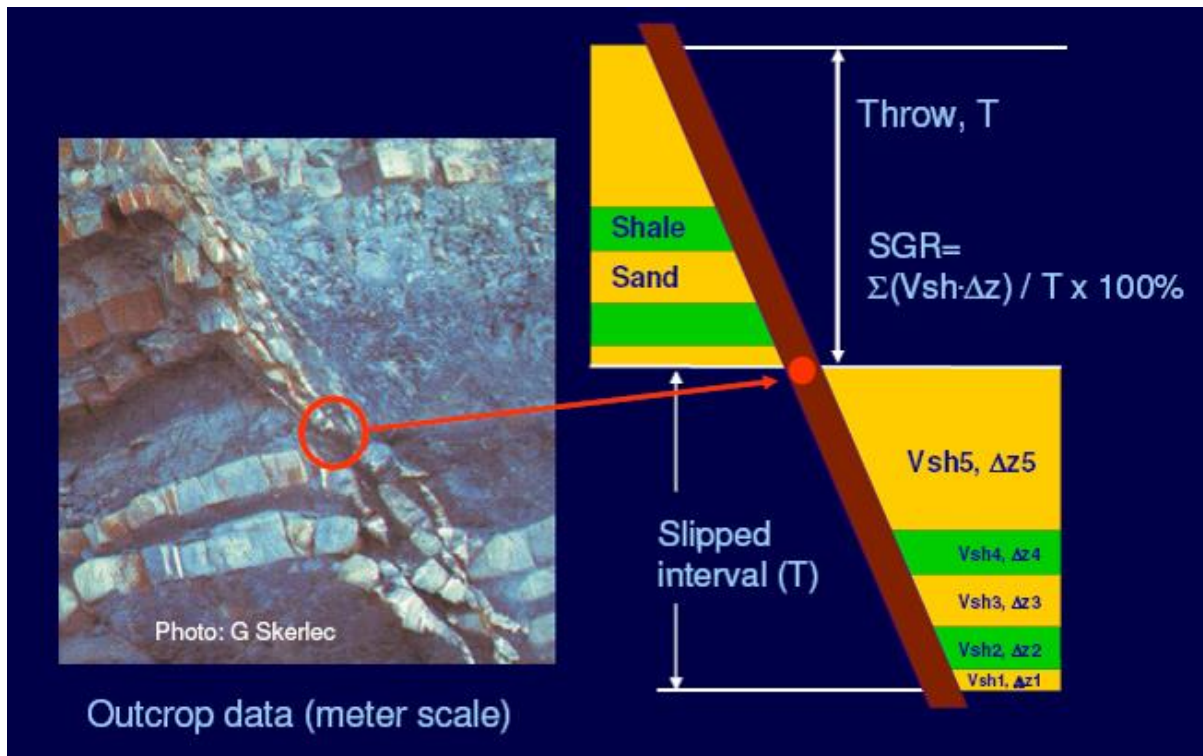


FIGURE 11. EXAMPLE OF SHALE GOUGE RATIO METHOD OF CALCULATION (YIELDING ET AL., 1997) WHERE VSH IS THE VOLUME OF SHALE EXPRESSED AS A % OF CLAY MINERALS IN A DISCRETE BED THICKNESS (Δz) AND T IS THE FAULT THROW.

6 Movement of Fluids in Faulted Rocks

Knowledge of the fault zone permeability allows an assessment of the capillary seal capacity for the fault (or the capillary pressure (P_c) that the fault is capable of supporting before the non-wetting phase can enter the fault pore space). For utilizing this relationship in pre-drill prediction of fault seal capacity, case examples of hydrocarbon pools thought to be controlled by capillary fault seal can be used to calibrate calculated SGR against measured across-fault pressure differences (ΔP_f). We can then use these same calibration techniques to predict fault permeability of other faults where there are no hydrocarbons trapped. The standard approach previously used for calculating ΔP_f is to use the pressure profile on either side of the fault and regardless of the fluid type (gas, oil or formation water), simply calculate the difference in pressure at a given elevation. Breton et al. (2003) presents an extensive pressure dataset from fields in globally distributed basins where the ΔP_f is plotted against the SGR. Fields are selected that are thought to be filled to their fault capillary seal capacity and where other components contributing to the total seal capacity are thought to be minor. Brown (2003) and Underschlutz (2007) identify that the distribution of formation pressure across the fault can have a significant contribution to the total seal capacity (explained in detail below) and this needs to be considered in the global ΔP_f – SGR calibration data. The presence of a water pressure differential across a fault also indicates, in itself, that the fault is of sufficiently low permeability to sustain that pressure gradient over time. Underschlutz (2007) provided a means to assess and correct global calibration datasets based on formation pressure distribution. Yielding et al. (2010) used the principles outlined in Underschlutz (2007) and revisited the global compilation of across fault pressure differences correlated with SGR (Breton et al., 2003) and applied a correction for those data that had sufficient information to do so. Yielding et al. (2010) discovered that the corrected data now define curved fault seal correlation envelopes that mimicked the theoretical curves derived by Sperrevik et al. (2002) from laboratory based experimentation. Several important implications are derived from Yielding et al. (2010):

- Above SGR values of ~0.5, further increase in SGR has progressively less impact on added seal capacity;

- At lower SGR values (the cut off value is dependent on fault depth), lateral seal capacity is effectively lost;
- There is general agreement between laboratory and field observations; and
- More robust global correlation data sets may further improve the definition of the seal capacity calibration envelopes (particularly at high and low SGR).

In order to evaluate fault zone permeability for input to regional groundwater models, a geological model is required that can estimate the volume of clay material in the stratigraphic layers either side of the fault. The fault throw distribution is also required and can be obtained from seismic data analysis. Finally the vertical formation pressure distribution is required on either side of the fault and this can be gained directly from multi-level monitoring bores or oil and gas wells with wireline test data or indirectly from formation water hydraulic head (H_w) distribution maps.

6.1 Multi-Phase Fluids and Capillarity

For the purpose of $SGR-\Delta P_f$ calibration, Underschultz (2007) shows that ΔP across the entire seal thickness (top seal or fault seal) has to be accounted for (not just the reservoir seal interface) or it could lead to an erroneous calibration. Schematic Figure 12A shows a simple trap geometry in order to demonstrate the principle of total seal capacity being effected by hydraulic head. A real fault will have a much more complicated permeability distribution. The reservoir, fault and top seal are considered isotropic and reservoir permeability (k_{res}) \gg fault zone permeability (k_{fz}) \gg top seal permeability (k_{ts}). Figure 12B and C consider the details of the reservoir adjacent to the fault with high H_w on the left and right sides respectively and each with a complementary capillary pressure curve for the fault rock.

In Figure 12B, H_w on the left side of the fault is higher than on the right. Once the hydrocarbon column reaches a height where the capillary pressure (P_c) is equal to the P_t of the capillary seal, the first pore of the fault is breached. Note that the H_w within the fault decreases towards the right; therefore once the first pore of the seal is breached, the hydrocarbon column has sufficient P_c to penetrate the entire fault zone. Also, in this example P_c never greatly exceeds the threshold pressure (P_t), thus the hydrocarbon saturation (S_h) within the fault zone remains low.

Figure 12C differs from the Figure 12B only in that the H_w on the left side of the fault is less than on the right. In this case, once the hydrocarbon column reaches a height such that the P_c is equal to the P_t , the first pore of the fault is breached. In order to breach the second and subsequent pores, however, the P_c must increase to match the increasing excess pore pressure within the fault zone. The higher H_w on the right side of the fault zone effectively increases the total capillary seal capacity (P_{tc}) allowing a larger hydrocarbon column to be trapped by the same permeability contrast. Under these conditions, note that the P_c required to breach the entire fault zone exceeds the P_t (by ΔP , the total increase in hydraulic head H_w across the fault zone) and thus it is expected that the hydrocarbon saturation S_h in the fault zone will be higher than in the previous case. Or in other words, the water saturation S_w will be lower, as gas and water saturation are related by $S_h + S_w = 1$.

While the theoretical examination of hydrodynamics and capillary seal capacity by Underschultz (2007) helps in the understanding of total fault seal capacity rather than just the P_t for a given permeability contrast, it only considers the case of hydrocarbons on one side of a fault. Underschultz (2007) limited the analysis to hydrocarbons on one side of the fault because it remained unclear if formation water pressure was likely to be transmitted through the hydrocarbon column at irreducible water saturation (S_{wi}). In recent years various authors (e.g. Teige et al., 2006; Moria 2011; Manzocchi and Childs 2013) have begun to address this question with current thinking suggesting that for water wet systems, the relative water permeability may become very small, but in practice never reach zero even towards the top of a hydrocarbon column.

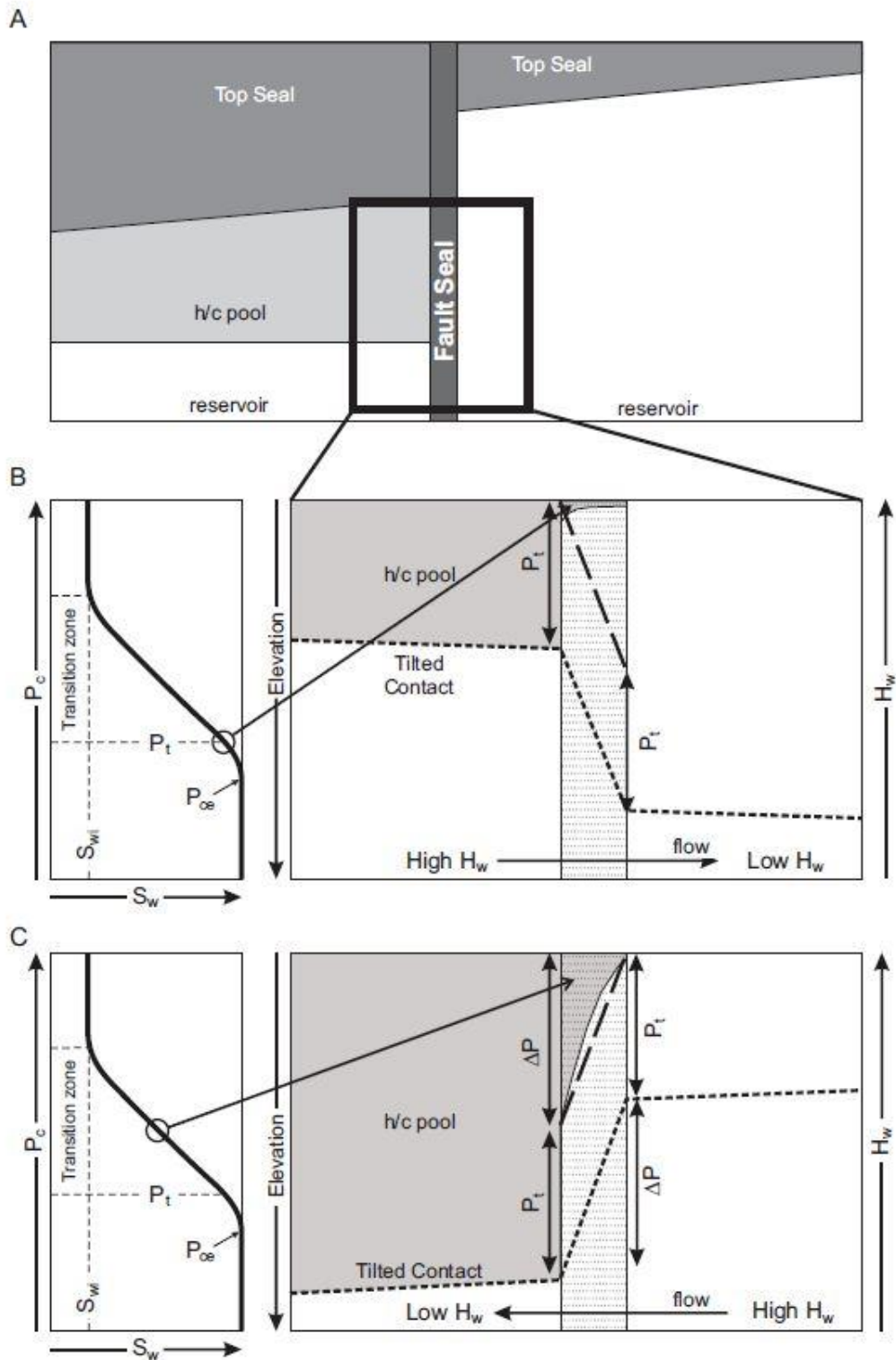


FIGURE 12. SCHEMATIC PRESENTATION OF A FAULT ZONE AT ITS CAPILLARY SEAL CAPACITY (A) TRAPPING A HYDROCARBON POOL. B AND C DEPICT A ZOOM IN OF THE FAULT ZONE-RESERVOIR INTERFACE UNDER DIFFERENT HYDRODYNAMIC CONDITIONS WITH A CORRESPONDING CAPILLARY PRESSURE CURVE OF THE FAULT ROCK IN QUESTION. THE ROCK PROPERTIES OF THE RESERVOIR AND FAULT SEAL ARE CONSTANT BUT THE TOTAL SEAL CAPACITY (P_{tc}) IS DEMONSTRATED TO CHANGE WHERE IN B) THE HYDROCARBON IS POOLED ON THE HIGH HYDRAULIC HEAD SIDE OF THE FAULT, AND IN C) THE HYDROCARBON IS POOLED ON THE LOW HYDRAULIC HEAD SIDE OF THE FAULT (UNDERSCHULTZ AND STRAND, 2016).

There has been debate in the literature regarding the implication of excess pressure (ΔP) and estimation of P_t for a seal using field data where a hydrocarbon pool is thought to be at the capillary seal capacity of its seal (Equation 1), and if modification to Equation (2) is required (Bjorkum et al. 1998; Clayton 1999; Rodgers 1999; Brown 2003; Teige et al. 2005; Moria 2011; Manzocchi and Childs 2013).

$$P_t = g\Delta ph \text{ (Equation 1)}$$

For our purpose here ΔP is considered the difference between the excess pressure in the aquifer below the free water level (FWL) and that within the first pores of the seal, Δp is the in situ density difference between the hydrocarbon and formation water, g is the gravitational constant and h is the height of the hydrocarbon column. In the case of fault seals, Brown (2003), and in the case of top seals, Clayton (1999), accept that towards the top of the hydrocarbon column, water saturation (S_w) approaches irreducible water saturation (S_{wi}) and relative permeability to water (k_{rw}) approaches zero. As a result, excess pressure (ΔP) must be incorporated into equation (2) as:

$$P_t = g\Delta ph - \Delta P \text{ (Equation 2)}$$

where ΔP is defined by the aquifer pressure on the opposite side of the seal (depicted graphically in Figure 13). Bjorkum et al. (1998) suggest that in a water-wet system, there exists a vertical water pressure gradient between the aquifer at the FWL and the top of the reservoir, even within the irreducible water phase and thus ΔP has no effect on calculated P_t . Rodgers (1999) pointed out that even if not zero, k_{rw} at the top of the reservoir would be much less than that in the aquifer, and that ΔP is still required to understand P_t (depicted at the seal-reservoir interface on Figure 13). Teige et al. 2005 suggest (based on one experiment with a highly permeable core plug) that the ΔP effect described by Rodgers (1999) is negligible. Teige et al. (2006) subsequently tested a range of plugs with variable reservoir properties and found that low permeability reservoirs at high P_c could sustain a significant ΔP effect as described by Rodgers (1999) but the core plug still transmitted water at low S_w . The results of Teige et al. (2006) imply that in some situations (e.g. low H_w on the opposite side of a seal from a low k_{res}) the P_{tc} will be reduced by the effect of ΔP at the reservoir-seal interface. Underschultz (2007) shows that seal breach needs to be considered across the entire seal thickness and that consideration of ΔP only at the reservoir-seal interface is insufficient. Figure 14 shows a schematic capillary pressure curve for both a reservoir and seal rock on the same plot. The reservoir rock only requires a small amount of P_c to significantly reduce the S_w but then a significant P_c is required to achieve S_{wi} . Once the hydrocarbon column is sufficiently large to induce a P_c equal to the P_t of the seal rock, the reservoir rock has a very low S_w but not S_{wi} . Teige et al. (2005 and 2006) found that k_{rw} in the reservoir rock remained higher than the k_{ts} required to hold back a hydrocarbon column of sufficient height to obtain the low S_w . Moria (2011) use an alternative adapted Mercury Injection Capillary Pressure (MICP) approach and concluded that the effective k_{rw} remained on the order of 10^{-2} to 10^{-3} mD even at several hundred metres above the FWL (assuming a water wet reservoir for the samples tested) independently corroborating the findings of Teige (2005 and 2006). It follows, that the capillary seal will typically be breached prior to the hydrocarbon column in the reservoir being large enough to reach S_{wi} . From the point of view of reservoir engineering that considers reservoir performance on the human time-scale, the semantics of S_w being very low but not absolutely S_{wi} is normally inconsequential and the assumption of S_{wi} is normally valid. When characterizing seal capacity and reservoir behaviour at the geological time-scales of trapping however, very low but non-zero k_{rw} has an important implication for predicting capillary seal capacity. With evidence mounting that the formation water phase likely transmits a continuous pressure gradient even for low degrees of water saturation (i.e. near S_{wi}), we can now take the results of Underschultz (2007) and extend them to other hydrocarbon fault seal cases that make up global fault seal calibration datasets even more robust (Underschultz and Strand, 2016). The notion of non-zero S_{wi} is of crucial importance for using SGR global calibration data to estimate fault zone permeability.

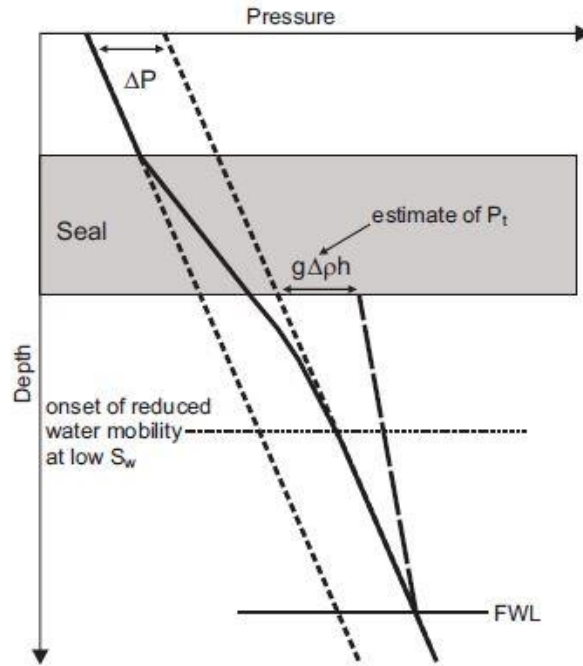


FIGURE 13. PRESSURE-DEPTH PLOT WITH A HYDROCARBON COLUMN EQUAL TO TOP SEAL P_t . IN THIS CASE P_t IS ESTIMATED TO BE THE DIFFERENCE IN THE HYDROCARBON AND WATER PRESSURE AT THE TOP OF THE COLUMN. ΔP IS THE EQUIVALENT PRESSURE DIFFERENCE BETWEEN H_w ON EITHER SIDE OF THE SEAL (AFTER RODGERS, 1999).

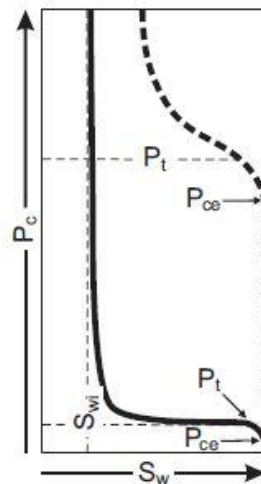


FIGURE 14. A SCHEMATIC CAPILLARY PRESSURE GRAPH PLOTTED AGAINST WATER SATURATION FOR BOTH A TYPICAL RESERVOIR (SOLID CURVE) AND SEAL ROCK (DASHED CURVE). P_{ce} IS THE CAPILLARY ENTRY PRESSURE AND P_t IS THE THRESHOLD PRESSURE. S_{wi} IS IRREDUCIBLE WATER SATURATION.

6.2 Consideration of Aquitards that are Hydrocarbon Wetting

It is interesting to note that in all of this report we consider systems where the hydrocarbon phase is assumed to be non-wetting. In unconventional reservoirs where the strata is both the source rock for the hydrocarbon and the reservoir, the reservoir itself is normally high in organic content and is often either mixed wetting or hydrocarbon wetting. This is true for most coal seam gas and shale gas reservoirs. In this case, the reservoir is normally very low permeability (acting as an aquitard) and the formation water is either mixed wetting or the non-wetting phase. Here the formation water must overcome capillary displacement pressure to migrate through the pore space. In the case of regional groundwater models, a regionally extensive unconventional gas

reservoir that is hydrocarbon wet has profound implications for hydraulic communication across these strata. Relative permeability curves for the groundwater need to be considered and implemented in a modelling code that can handle multiphase flow. These data are normally obtained in laboratory experiments using core plug samples. Since absolute permeability is highly variable, the relative permeability values are too; meaning that a large number of samples are required to gain confidence that the permeability is adequately represented. Both the American Association of Petroleum Geologists and the Society of Petroleum Engineers are professional organisations that host web sites with general background information on “wettability” and “relative permeability” that serve as general references⁶⁷⁸. Historical early references to wettability and relative permeability include Corey (1955) and Brooks and Cory (1966). There are a number of laboratory procedures that can be employed to measure relative permeability on core samples as described by Josh et al. (2012), Pini and Benson (2013) and Donaldson and Alam (2013).

7 Case Studies and Conceptual Flow Models in Faulted Rock

It is extremely rare to have sub-surface hydrodynamic data (formation pressure, temperature, or fluid chemistry) from within a fault zone (a notable exception is Seebeck et al. (2014)). As such, in order to use our theoretical knowledge of fluid behaviour within various fault zone architectures under certain conditions of stress, we need to derive conceptual hydrodynamic models grounded in hydrodynamic data that are located in the vicinity of faults. With a characterisation of the fault zone physical characteristics and an appropriate conceptual hydrodynamic model, we can then have a process to constrain a realistic interpretation of the fault zone hydraulic characteristics to be upscaled into a regional groundwater model. In this section we use case study examples to illustrate how a well-informed conceptual hydrodynamic model of faulted strata can be developed. We draw on the public domain literature for examples of how others have approached this problem and many of these involve conventional hydrocarbon pools as part of the characterisation. As stated earlier, often the motivation for these studies is to better understand the seal performance of retaining hydrocarbons in conventional faulted reservoirs, however to do this all methods ultimately rely on a characterisation of the fault rock property prediction. For this reason, it is appropriate to use the same approaches and techniques and apply them in the context of unconventional reservoirs to understand the role of faults in unconventional gas development and how faults may influence cumulative effects of adjacent aquifers. Armed with methodology for characterising fault zone rock properties we then have the basis of up-scaling representative fault zone hydraulic characteristics to parameterise regional groundwater models.

Standard hydrodynamic approaches to characterizing flow systems in unfaulted confined aquifers include the analysis of pressure data, both in vertical profile (e.g. pressure-elevation plot), and within the plane of the aquifer after conversion to hydraulic head. Monitoring bore data can also be used if water level data is corrected for density effects. All data of course need to pass through a quality assurance process. Pressure data are supplemented with formation water analysis and formation temperature data to aid in the evaluation of the flow system. Bachu and Michael (2002), Otto et al. (2001), Bachu (1995), and Dahlberg (1995) provide an overview of hydrodynamic analysis techniques. Evaluation techniques for the culling and analysis of formation water samples are described by Underschultz et al. (2002), and Hitchon and Brulotte (1994). Techniques for the evaluation of formation temperature are described by Bachu et al. (1995), and Bachu and Burwash (1991).

The characterization of formation pressure in faulted aquifers requires careful analysis. Inferences about the fault zone hydraulic characteristics need to be made by evaluating formation pressure data from reservoir or aquifer quality rock adjacent to the fault. Yassir and Otto (1997) and Underschultz et al. (2005) describe some theoretical patterns of H_w in faulted aquifers for various flow conditions, and pressure gradients on pressure elevation plots for faults with various hydraulic properties. For faulted aquifers, the hydraulic head distribution is first characterised in unfaulted blocks of the aquifer. Then the hydraulic head distributions in adjacent blocks

⁶ http://wiki.aapg.org/Relative_permeability

⁷ <http://wiki.aapg.org/Wettability>

⁸ http://petrowiki.org/Relative_permeability

are compared, and built as a patchwork into a flow model that is representative of the faulted strata as a whole (Underschultz et al. 2005, and Underschultz et al. 2003). At this stage the patterns in both hydraulic head and formation water chemistry or formation temperature can be assessed relative to the theoretical distributions one would expect given certain fault sealing or conduit characteristics.

Underschultz et al. (2005) describe that if a fault is acting as a conduit, with higher permeability along the fault than the aquifer it crosscuts, and if the fault zone permeability pathway is vertically continuous to either a separate aquifer or the land surface (or seabed), then the aquifer will “see” the fault as either a source or a sink for fluids. The hydraulic head distribution in the aquifer will form either a closed high or low against the fault surface, indicating that formation water is either emanating from the fault zone into the aquifer (fault = source) or flowing from the aquifer into the fault zone (fault = sink), respectively (Figure 15a). This analysis can be supplemented by evidence such as thermal springs at the land surface or pock marks and seeps on the sea floor (Talukder et al. 2013), or thermal and chemical anomalies of the formation water in the aquifer adjacent to the fault. If, for example, a fault zone is acting as a conduit recharging an aquifer at depth, it is expected that the formation water in the aquifer would be relatively fresh and have a meteoric ionic signature, such as elevated HCO_3 and/or SO_4 . The likelihood of an aquifer being in hydraulic communication with the land surface can be deduced by comparing the hydraulic head in the aquifer with the elevation of the water table (commonly similar to the topographic elevation in many parts of the world but in arid regions such as parts of Australia this may not be true). If the hydraulic head in the aquifer is similar to the water table elevation, it is possible that the water table elevation is in hydraulic communication with the aquifer.

At any one location, the vertical hydraulic communication can be examined by pressure-elevation plot analysis. If two vertically separated aquifers are in hydraulic communication via a fault zone conduit, the pressure data from the two aquifers near the fault should define a near-common hydrostatic gradient on a pressure-elevation plot (Figure 15b). In this schematic example, the hydraulic head in the deeper aquifer is slightly higher than the shallower aquifer, which allows for the flow up the fault zone. For this reason, the Wire Line Test (WLT) pressure data in aquifer 2 fall slightly above the pressure gradient defined by the data in aquifer 1 on the pressure-elevation plot (Figure 15b). It should be noted that vertical continuity of a hydrostatic pressure gradient between two aquifers may also simply be coincidental. This observation on its own is not conclusive evidence of vertical hydraulic communication between the two zones. It also assumes that pressures being observed are pre-production. Even if on geological time-scales there is hydraulic communication, a pressure transient induced by producing one aquifer will take some time (dependent on the permeability and cross sectional area) to propagate up a fault to another aquifer level.

An actual example of this type of fault characteristic resulting in a closed hydraulic head high or low against a fault intersecting an aquifer can be seen in Figure 16. In this case there is a discontinuity in hydraulic head across the Challis field bounding fault with lower values on the north side. On the south side of the fault there is a closed hydraulic head high against the field bounding fault indicating the formation water is migrating up the fault and then out into the Challis aquifer migrating to the south underneath the hydrocarbon accumulation.

When a fault zone has lower permeability than the aquifer it crosscuts, the flow direction in the aquifer adjacent to the fault will tend to be parallel to the plane of the fault (Figure 17a). This nature of the flow often leads to a relatively abrupt contrast in hydraulic head values in the aquifer directly across the fault (a hydraulic head discontinuity). The more significant the fault is as a barrier, either because of juxtaposition or low fault rock permeability, the more severe the hydraulic head discontinuity potentially could be, although this is not a necessary criterion. In this schematic example (Figure 17a), there is a 70 m drop in hydraulic head across the fault zone. If the fault zone could be examined at a small scale, the discontinuity in hydraulic head would actually be a very steep hydraulic head gradient along the plane of the fault (see Figure 18), thus leading to some leakage across the fault plane, but the flux would be negligible compared to that moving parallel to the fault plane in the adjacent aquifer. Figure 18 shows a schematic cross section perpendicular to a sealing fault. In this direction there is a hydraulic gradient from right to left with a steep gradient through the fault. The flux through the fault will be relatively small due to the low permeability whilst in and out of the line of section the flux will be relatively higher. The shape of the hydraulic head contours through the hydrocarbon reservoir demonstrates the effect of the reducing relative permeability to the water phase with height up the hydrocarbon column (see Figure 13 and Figure 14 as discussed previously). Corroborating evidence for fault zone barriers are the accumulations of hydrocarbon on one side of the fault, and discontinuities in the formation water chemistry across the fault. At any one location, the vertical hydraulic communication can be examined by pressure-elevation plot analysis for a well near to, or crosscut by a fault (b). Zones of low hydraulic transmissivity manifest themselves as a break in the observed pressure gradient with depth (Dahlberg, 1995).

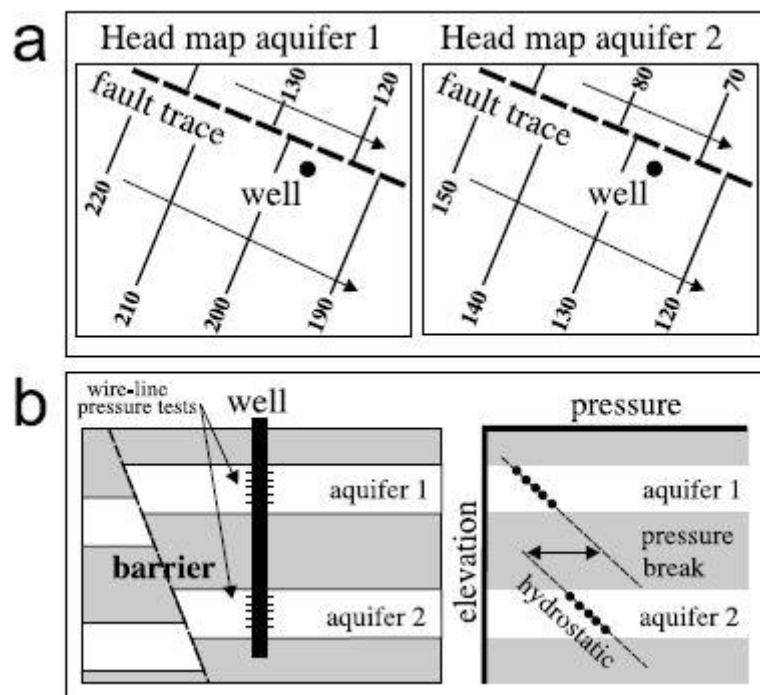


FIGURE 17. SCHEMATIC FAULT HYDRODYNAMICS (MODIFIED FROM OTTO ET AL., 2001). (A) HYDRAULIC HEAD DISTRIBUTIONS IN TWO STACKED AQUIFERS CROSSCUT BY A BARRIER FAULT; AND (B) CROSS SECTION OF THE BARRIER FAULT IN (A) WITH NO UPFAULT FLOW AND THE CORRESPONDING PRESSURE-ELEVATION PLOT OF WLT DATA FROM THE TWO AQUIFERS AT THE WELL LOCATION. UNDERSCHULTZ ET AL. (2005)

There are multiple case study examples of faults compartmentalising aquifers where the hydraulic head is represented as a discontinuity. Figure 19 shows an example of regionally mapped hydraulic head in faulted Plover strata in the Vulcan sub-basin (Underschultz et al. 2002). Similarly, Figure 20 is a hydraulic head distribution mapped for the Barrow aquifer in the vicinity of the Pyrenese-Macedon oil and gas fields (Bailey et al. 2006). In these cases, accurate understanding of the hydraulic head and seal capacity allows for predictive

estimation of hydrocarbon pressure distributions, hydrocarbon compartmentalisation and reservoir performance that can be calibrated with historical production data. The notion of hydraulic connectivity and fault architecture also relates to how strain is transferred from one fault to the next through what are normally described as relay ramps (Figure 21). These relay ramps can provide a path of hydraulic continuity that can be mapped (Bense and Van Balen, 2004) in terms of hydraulic head (Figure 22).

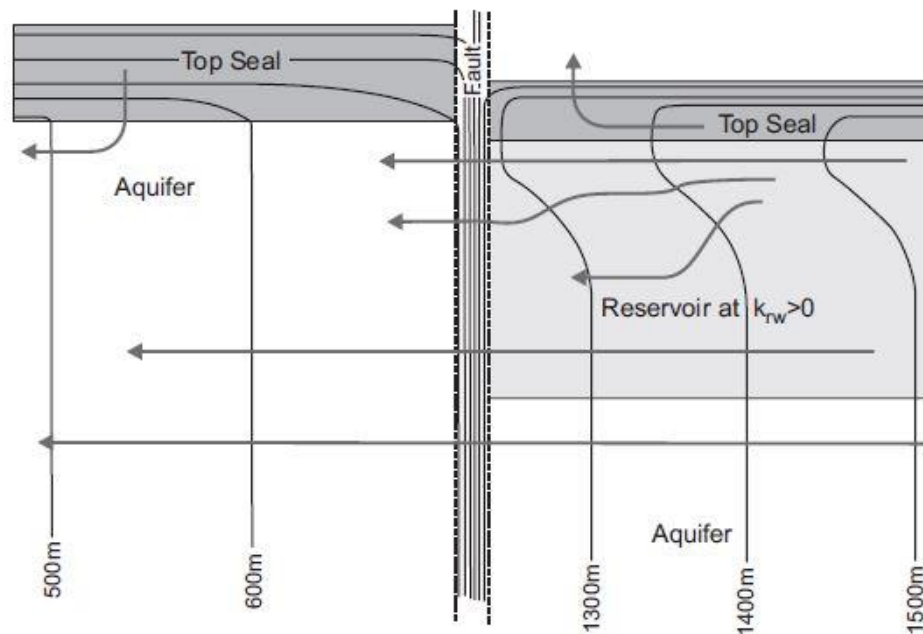


FIGURE 18. SCHEMATIC CROSS SECTION ACROSS A SEALING FAULT WITH A THEORETICAL HYDRAULIC HEAD DISTRIBUTION (BLACK CONTOURS LINES) IN THIS DIMENSION. FLOW PATHS ARE MARKED WITH ARROWS. THE BULK OF THE FLUX IS LIKELY OCCURRING PERPENDICULAR TO THE LINE OF SECTION BECAUSE THE FAULT ZONE HAS A VERY LOW PERMEABILITY RESULTING IN THE TIGHT HYDRAULIC HEAD GRADIENT.

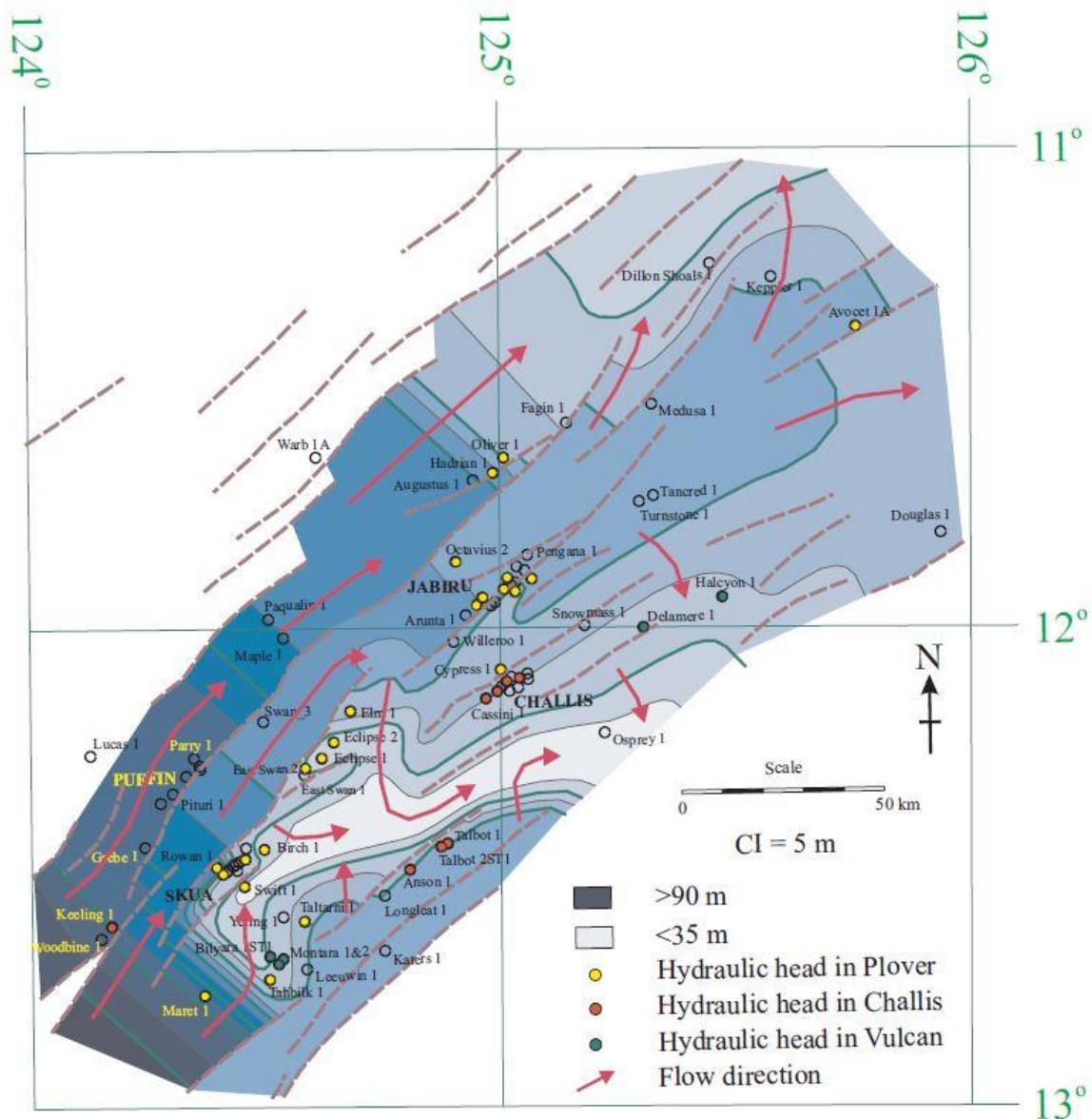


FIGURE 19. FRESH-WATER HYDRAULIC HEAD (M) DISTRIBUTION FOR THE PLOVER AQUIFER SYSTEM, VULCAN SUB-BASIN (UNDERSCHULTZ ET AL. 2002).

Hydraulic head discontinuity is however not restricted to the deep subsurface. Bense and Van Balen (2004) examined shallow groundwater systems in the lower Rhine Graben of the Roer Valley Graben and they noticed hydraulic head discontinuities controlled by fault distributions (Figure 23). Here the faults appear to be acting mainly as barriers where hydraulic head discontinuities occur across fault traces and flow is parallel to the fault trace.

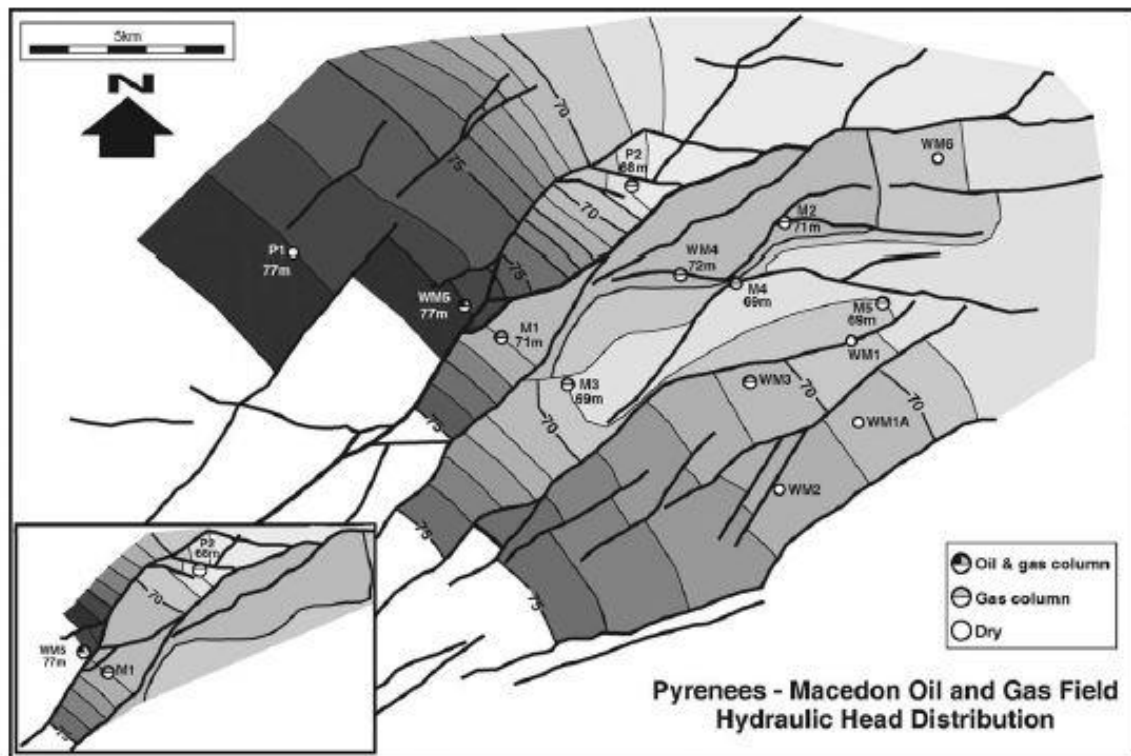


FIGURE 20. HYDRAULIC HEAD DISTRIBUTION MAP FOR THE BARROW AQUIFER FOR THE P–M FIELDS. INSET SHOWS ALTERNATIVE INTERPRETATION FOR HEAD DISTRIBUTION IN THE COMPARTMENT BETWEEN PYRENEES-2 AND WEST MUIRON-5. GREY SHADING THAT DEFINE THE CONTOURS REPRESENTING FRESH WATER HYDRAULIC HEAD (M). HEAVY BLACK LINES REPRESENT MAJOR FAULT TRACES (BAILEY ET AL. 2006).

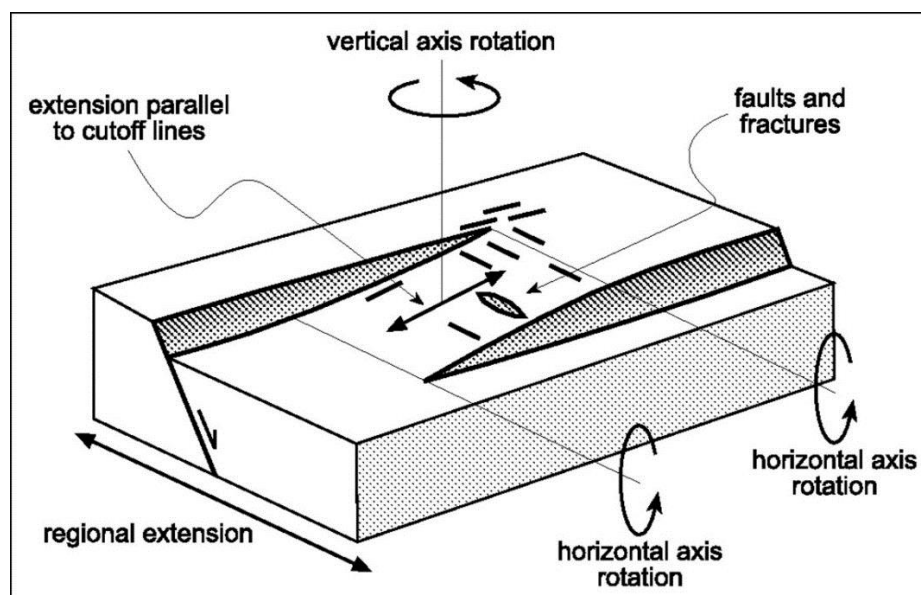


FIGURE 21. A SCHEMATIC DIAGRAM OF THE MAIN FEATURES OF A STRUCTURAL RELAY RAMP (DI BUCCI ET AL. 2006).

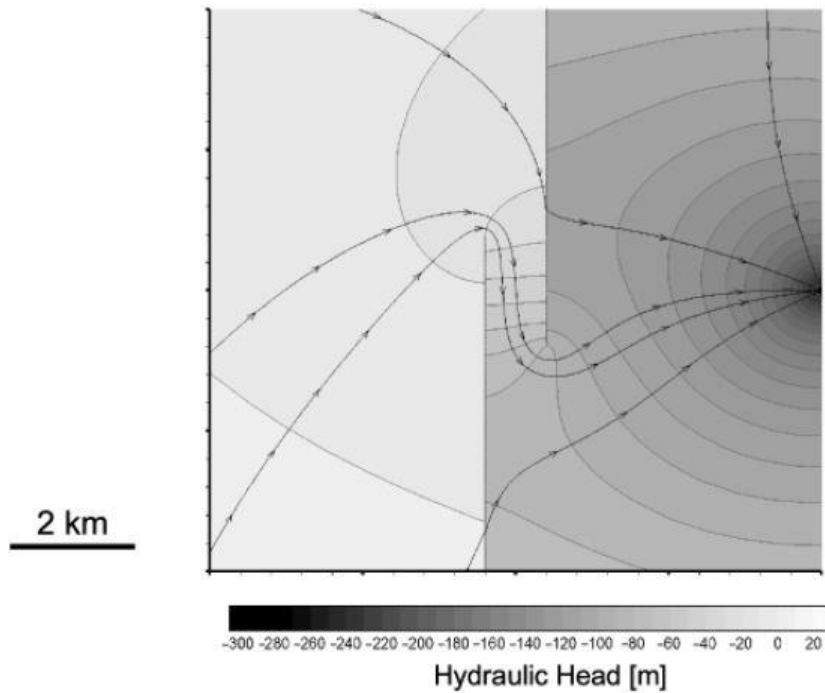


FIGURE 22. DETAIL OF THE MODEL SHOWING THE GROUNDWATER FLOW PATTERNS (BLACK LINES WITH ARROWS) AROUND THE FAULT RELAY. CONTOUR INTERVAL IS 10M (BENSE AND VAN BALEN 2004).

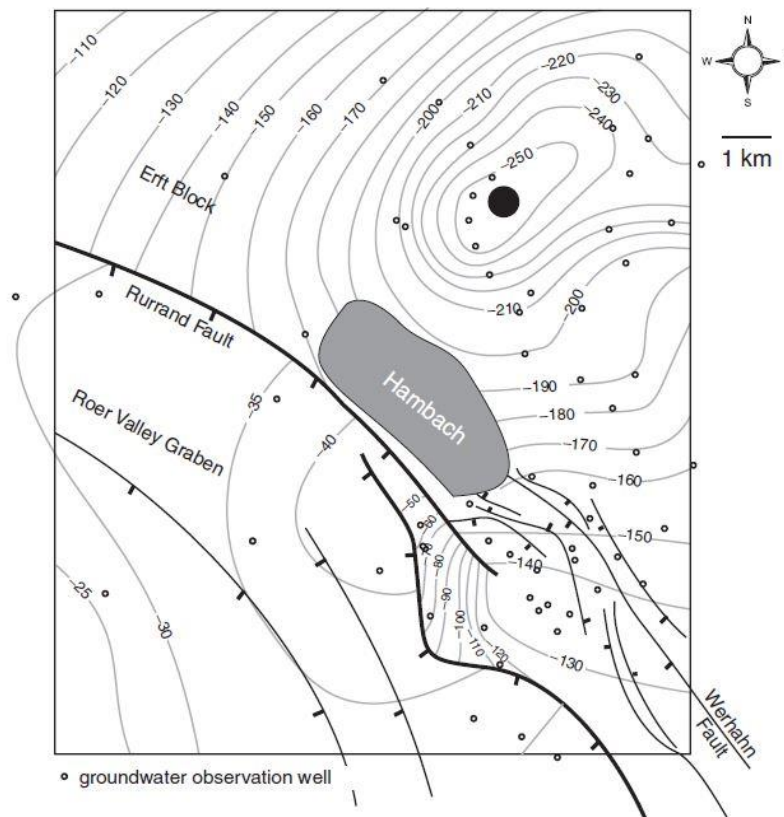


FIGURE 23. HYDRAULIC HEAD IN A SHALLOW AQUIFER OF THE LOWER RHINE EMBAYMENT OF THE ROER VALLEY GRABEN. CONTOUR LINES ARE FRESH WATER HYDRAULIC HEAD (M) AND HEAVY BLACK LINES WITH TICK MARKS ARE MAJOR FAULT TRACES. WELL LOCATIONS ARE INDICATED BY OPEN CIRCLES (BENSE AND VAN BALEN, 2004).

Similarly, hydraulic head and salinity distribution in the foothills of the Western Canadian Sedimentary basin mapped by Underschultz et al. (2005) show compartmentalisation and hydraulic head discontinuities across thrust faults that displace Mississippian strata, but vertical hydraulic communication at lateral ramps with faults acting as conduits creating vertical transmissivity between Mississippian and Devonian aquifers. This data is also supported by the location of thermal springs at some lateral ramp locations. In this case, the fault zone orientation relative to the prevailing stress regime correlates to sealing and dilatant fault segments. Finally, Figure 24 also shows the en-echelon fault architecture in the foothills east of the Rocky Mountain main ranges and the nature of flow systems in this region where hydraulic continuity is achieved around fault tips where strain is shifted to the next sub-parallel fault. A schematic NW-SE oriented cross-section of the Brazeau thrust sheet across the lateral ramp that terminates its extent (see Figure 24) is displayed in Figure 25. It demonstrates the geometry of the flow systems (head and salinity) in the Mississippian and Devonian Woodbend aquifers in relation to the lateral ramp.

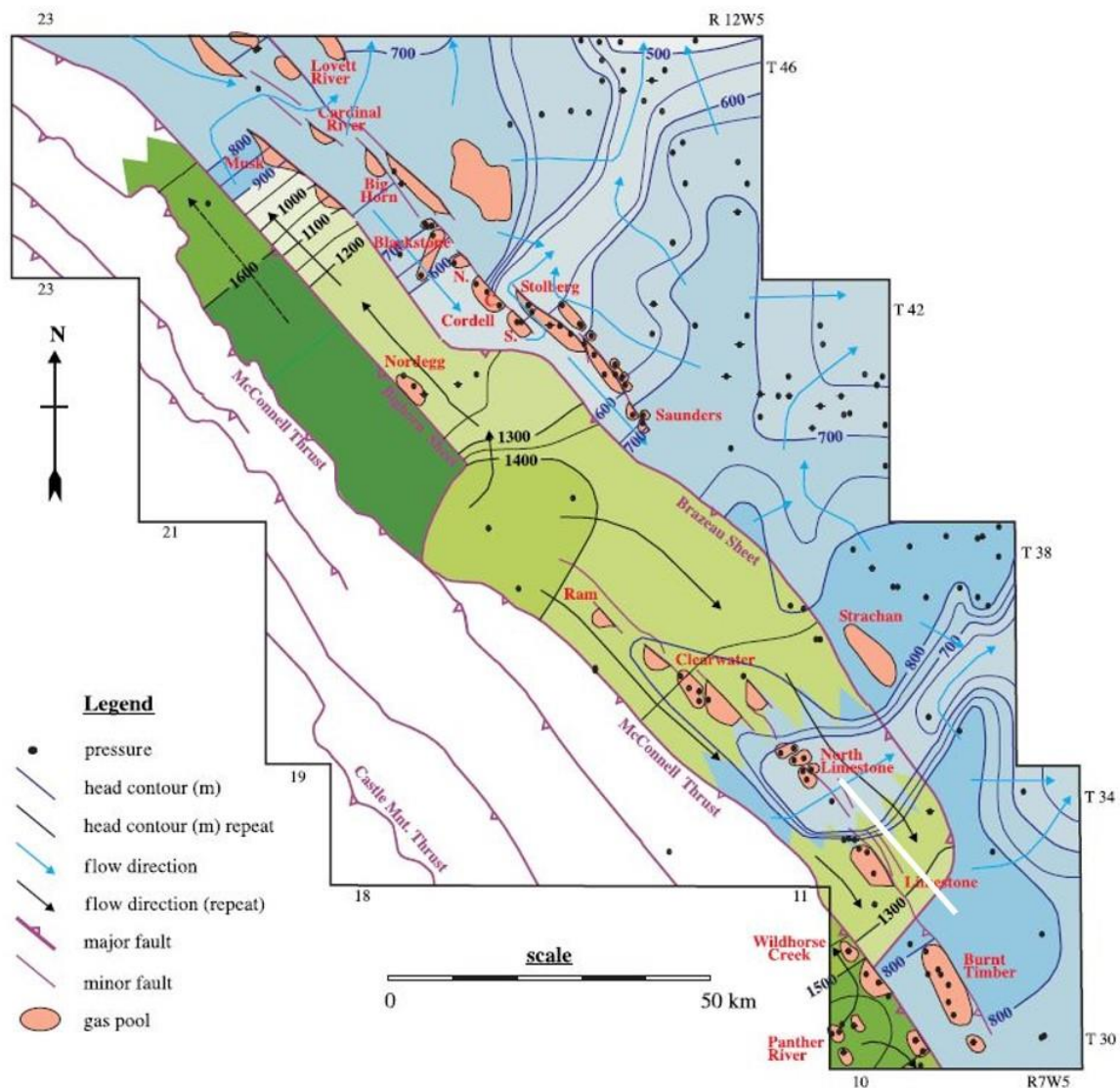


FIGURE 24. HYDRAULIC HEAD (M) DISTRIBUTION FOR THE MISSISSIPPIAN AQUIFER WESTERN CANADA (UNDERSCHULTZ ET AL. 2005). THE WHITE LINE IN THE SE CORNER OF THE MAP IS THE LOCATION OF THE CROSS SECTION DEPICTED IN FIGURE 25 TO FOLLOW.

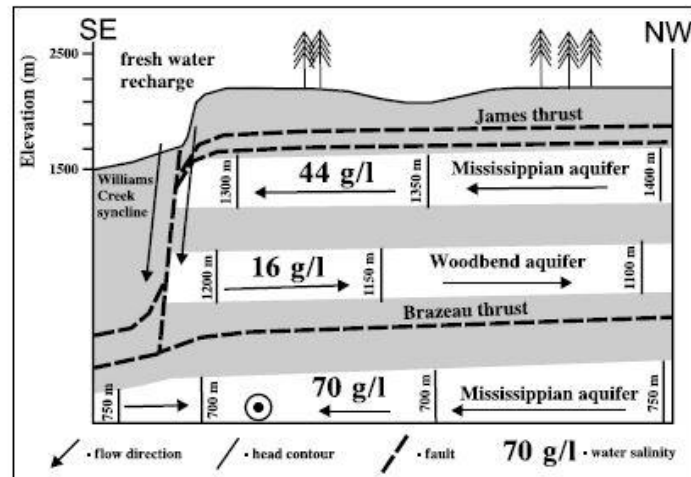


FIGURE 25. SCHEMATIC STRIKE CROSS SECTION OF THE BRAZEAU THRUST SHEET (UNDERSCHULTZ ET AL. 2005, BASED ON BEGIN AND SPRATT, 2002) THE LOCATION OF WHICH IS MARKED BY A WHITE LINE IN THE SE CORNER OF FIGURE 24..

While Underschultz et al. (2005) considers both head and salinity data, Bense et al. (2013) describe temperature anomalies associated with up and down fault flow systems (Figure 26). The distribution of multiple independent data sets each associated with the flux of formation water can be utilised to decipher flow system geometry in the vicinity of fault systems.

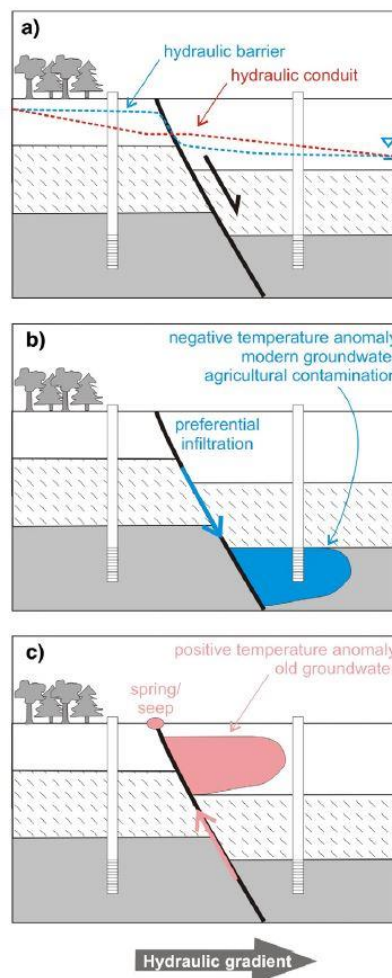


FIGURE 26. SHALLOW FAULT ZONE WITH A) WATER LEVEL SCENARIOS, AND B) AND C) NEGATIVE AND POSITIVE THERMAL ANOMALIES RESPECTIVELY. (BENSE ET AL. 2013).

This section described the issue of scale in representing hydraulic head distributions (and other parameters such as formation water chemistry and formation temperature) in faulted strata. Even though in reality the distribution of these parameters is represented by a continuum, at regional scale this is often not possible to capture and we revert to representing these parameters as a discontinuity across faults. This is simply because there may be such steep gradients within the thickness of the fault zone that it is not possible to depict at regional scale. A numerical simulation however needs to accommodate this continuity in some way. Strategies such as nested model grid refinement may provide at least partial solutions.

8 Groundwater Springs and Faults

Groundwater springs have been a topic of interest to humans for millennia as they mysteriously emanate from rocks or sediments and provide a source of water at ground surface (Fensham et al., 2014). A major category of research and reporting concerns the occurrence of groundwater springs located along faults that come to surface. In the Australian context there has been substantial work conducted on classifying and studying springs of the GAB. (Habermehl, 1982) describes faults as being one of three categories to classify the origin of GAB springs and describes the first artesian bores drilled in New South Wales and South Australia (in the south and southwest part of the GAB) to be located near springs. By examining the temperature of the spring it is possible to consider the depth from which the formation water comes under various permeability assumptions (Lopez & Smith, 1995). If temperature observations are coupled with geochemistry, the prediction of circulation depth can be even more accurately estimated (Grasby & Hutcheon, 2001). Even further constraints can be gained by examining isotopic data (Keppel et al., 2013). Other researchers considered the state of stress and fault zone geometry and related this to the flux of observed groundwater spring discharge at surface (Gudmundsson, 2000) and further observed that seismically active faults coincide with variable spring discharge rates coincident with slip events. In the Surat Basin the Office of Groundwater Impact Assessment has done extensive work on understanding springs and the risk of impact from coal seam gas development (Queensland-Water-Commission, 2012). The work on springs provides us with two useful results: 1) there is plenty of evidence that under certain conditions, faults can provide hydraulic conduits to surface capable of significant flux, and 2) the measurement of spring temperature, geochemistry and isotopic signatures can provide valuable calibration data to constrain fault zone hydraulic parameters and rock properties. Regional groundwater models extended to include solute transport capability that incorporate fault zone hydraulic properties can be calibrated and/or validated against the flux and geochemistry of observed springs.

9 More Detailed Fault Representations

In the examples of flow systems geometries in the vicinity of faults that have been shown thus far, the fault zone itself is generally represented as a plane. Faults in the subsurface are represented as simplistic planar surfaces because there is normally not enough information (wells or seismic) to understand and represent more complexity than that. The reality is that fault systems can be much more complex and it is important to consider if a simplistic realisation misrepresents the hydraulic processes that are actually occurring. This can be grounded in outcrop analogues where faults are exposed and we can observe the range of detailed strain that may occur in various scenarios of deformation. Through this consideration there could be insights to up-scaling considerations that will be important for incorporating fault zone hydraulic characteristics in regional groundwater flow models.

Bense et al. (2013) focuses on characterising faults in shallow aquifer systems. Figure 27 describes the type of information one might have at surface in observations of fracture permeability and how this might relate to faulting at depth. They describe how this might compare to information accessible from bore holes at depth. This difference in detail of information relates to how faults are often treated in numerical simulations. Bense et al. (2013) then consider the distribution of fracture permeability more holistically both in the damage zone and how that relates to the clay smear in the fault core (Figure 28). This distribution can be related to the amount of throw on the fault at the location of interest. Bense et al. (2013) also correlate the representative permeability profile across the damage and fault core zones of a fault. With this distribution one then considers that a fault could have a core that prevents across fault hydraulic communication however the higher permeability of the adjacent damage zone may enhance flux laterally and vertically parallel to the fault plane core potentially providing vertical hydraulic communication. Figure 28 does not, however, consider the implications of these observations in regard to the fault continuing up through a top seal that has different

rheology. It only considers the parameterisation of this complicated fault zone geometry within aquifer (reservoir) rock. Bense et al. (2013) extend this characterisation to a multi-layered system of inter bedded aquifer and aquitard lithologies (Figure 29).

Depending on depth of the fault zone and rheology of the rock framework, Bense et al. (2013) demonstrate how the distribution of the fault core and the damage zone can be expected to be developed. They also indicate the relative permeability ellipse that can be associated with each of the zones. In addition, one might expect that the situation described by Bense et al. (2013) will also be dependent on the throw of the fault. It raises the question of how this complicated distribution of fault zone permeability could be up-scaled and represented in a meaningful way in regional groundwater flow models. In the case of CSG reservoir development and impacts on adjacent aquifer systems, just considering the permeability distribution of these complex systems may not be sufficient. The relative permeability and the associated capillary forces may also need to be considered in the case of gas transport.

Seebeck et al (2014) have made further advances in considering the details of fault zone architecture and how this relates to hydraulic properties. They examined faults in New Zealand that had been instrumented to estimate fluxes of water in different locations of the fault. Figure 30 shows a sample of a complicated fault zone architecture and the distribution formation water flux where “fault and fracture networks capable of sustaining low to moderate ($<5 \times 10^3 \text{ m}^3/\text{s}$) and high ($>5 \times 10^3 \text{ m}^3/\text{s}$) flow rates shown by light and dark blue shading, respectively. The location, rate, and direction of flow (red filled circles and arrows) in this study is considered a function of the proximity to primary slip surfaces (zones) and the connectivity of a fault and fractures to other hydraulically conductive elements within the groundwater system. The connectivity of the network is largely controlled by the longest faults”.

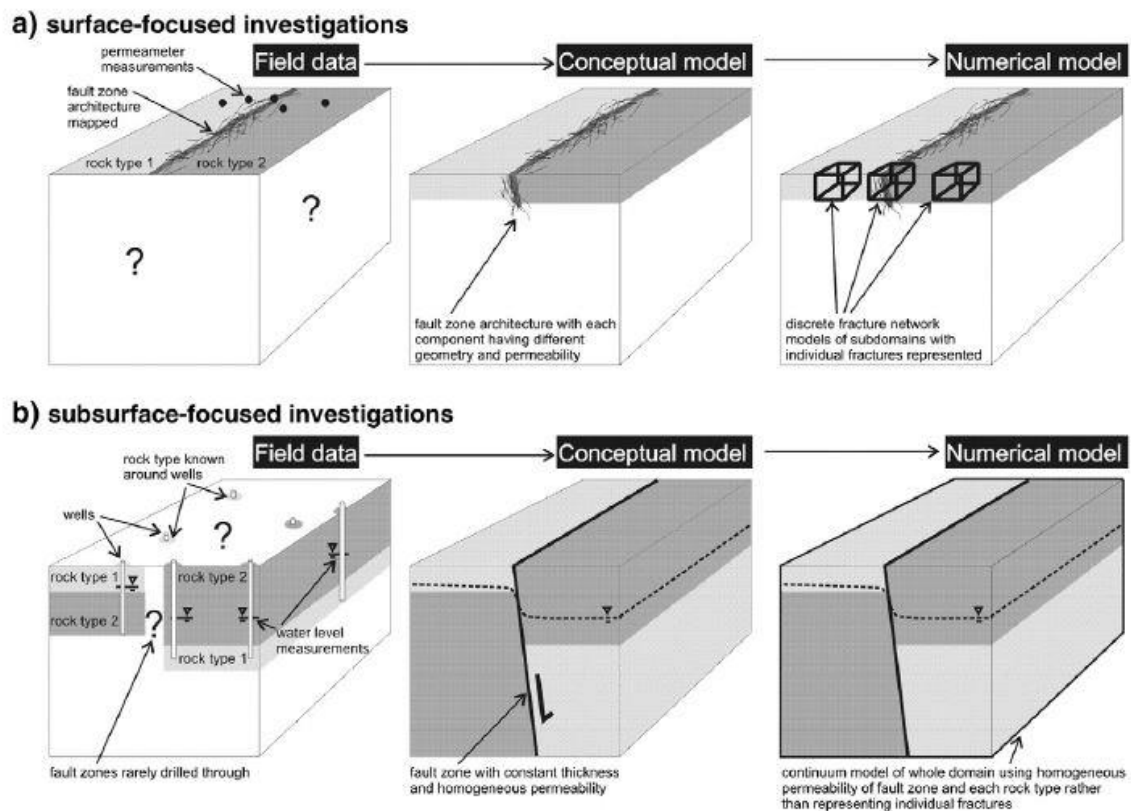


FIGURE 27. COMPLEX FAULT ZONE HYDROGEOLOGY FOR A SHALLOW AQUIFER HORIZON WHERE A) SHOWS SURFACE FOCUSED INVESTIGATIONS AND B) SHOWS SUBSURFACE FOCUSED INVESTIGATIONS (BENSE ET AL. 2013).

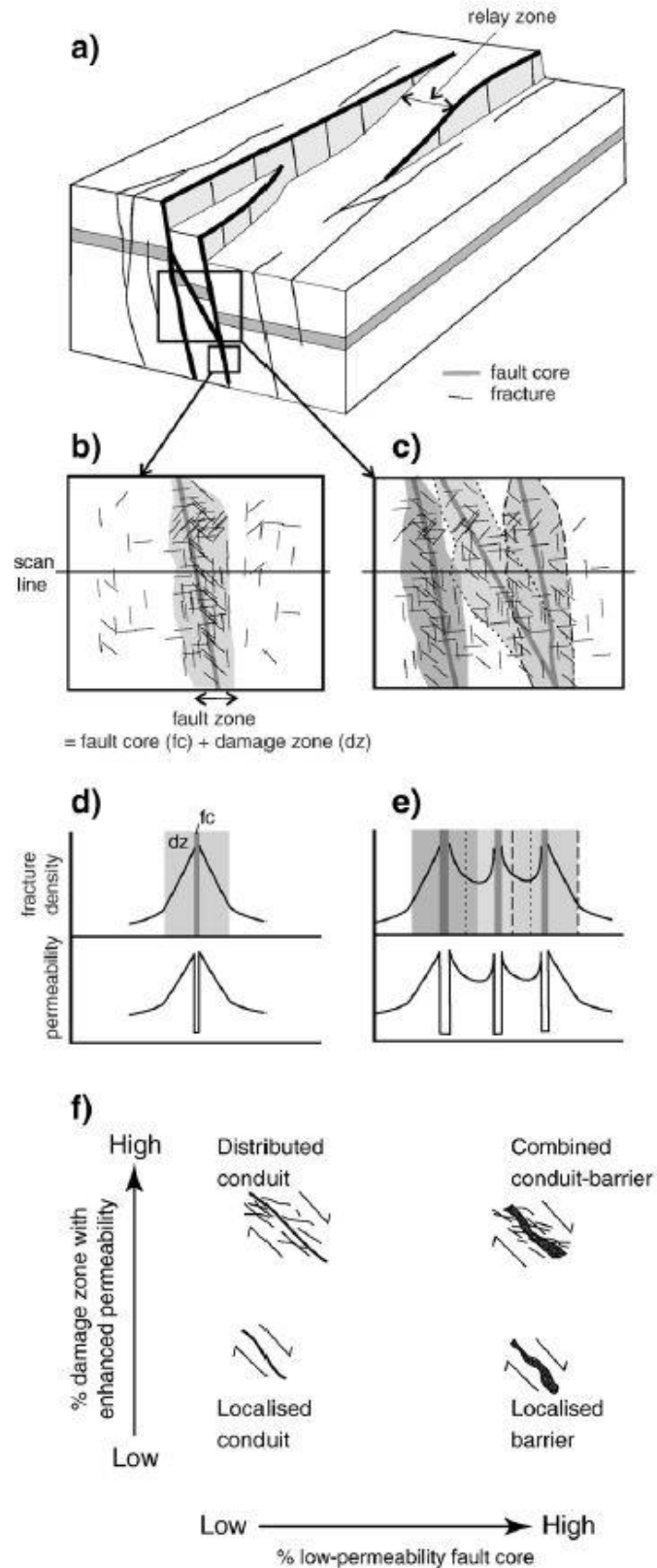


FIGURE 28. COMPLEX FAULT ZONE HYDROGEOLOGY FOR AN AQUIFER HORIZON WHERE A) IS A BLOCK MODEL, B) IS A DETAILED SCAN THROUGH ONE FAULT CORE, C) IS A DETAILED SCAN LINE THROUGH THREE FAULT CORES, D) IS THE FRACTURE DENSITY AND PERMEABILITY DISTRIBUTION ON SCAN LINE B, E) IS THE FRACTURE DENSITY AND PERMEABILITY DISTRIBUTION ON SCAN LINE C, AND F) CATEGORISATION MATRIX OF DAMAGE ZONE WIDTH VS. PERMEABILITY OF FAULT CORE INTO FLOW CHARACTERISTICS (BENSE ET AL. 2013).

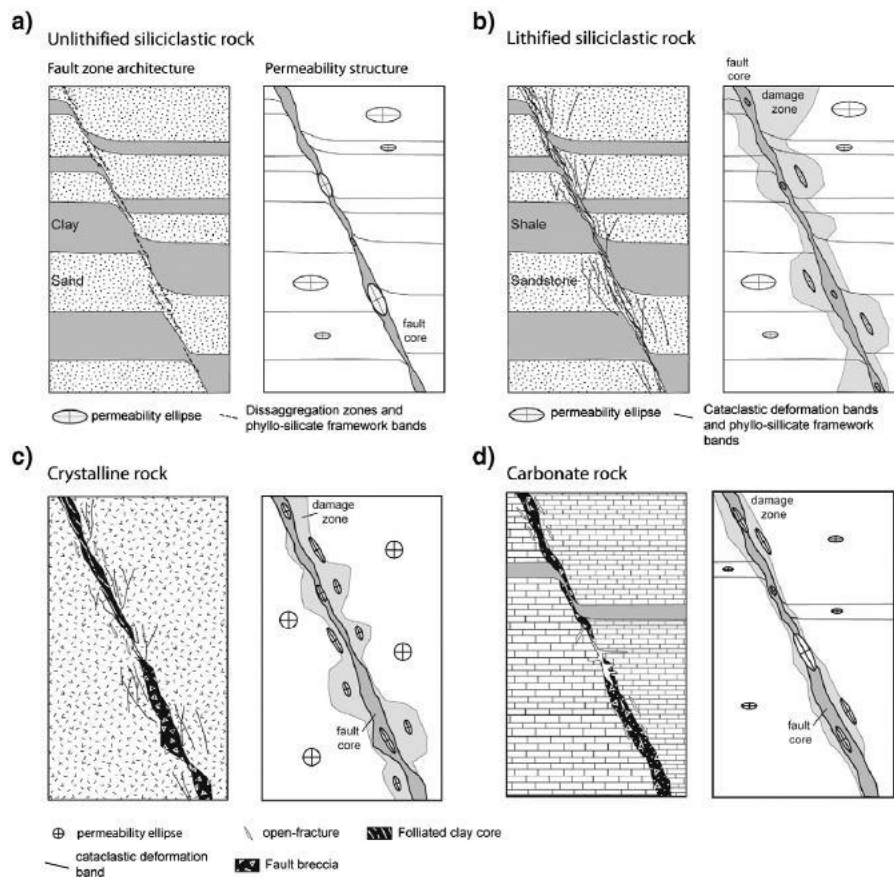


FIGURE 29. COMPLEX FAULT ZONE HYDROGEOLOGY FOR AN INTERBEDDED SEQUENCE OF AQUIFERS AND AQUITARDS WHERE A) UNLITHIFIED SILICICLASTIC RHEOLOGY, B IS LITHIFIED SILICICLASTIC RHEOLOGY, C IS CRYSTALLINE ROCK RHEOLOGY, AND D) IS CARBONATE ROCK RHEOLOGY (BENSE ET AL. 2013).

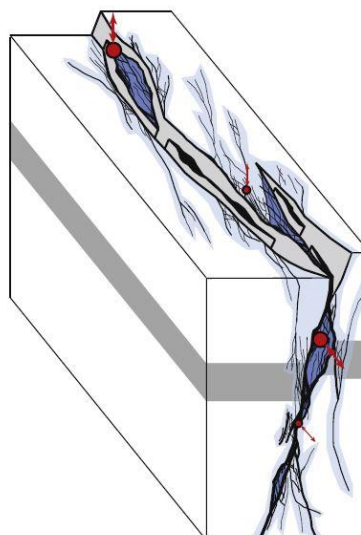


FIGURE 30. FLUID FLOW IN FAULT ZONES FROM AN ACTIVE RIFT. GEOMETRY OF THE DETAILED FAULT ZONE ARCHITECTURE RELATED TO THE FLUX DISTRIBUTION OF FORMATION WATER WHERE LOW TO MODERATE ($<5 \times 10^3 \text{ m}^3/\text{s}$) AND HIGH ($>5 \times 10^3 \text{ m}^3/\text{s}$) FLOW RATES SHOWN BY LIGHT AND DARK BLUE SHADING, RESPECTIVELY. THE RED DOTS SHOW LOCATION AND DIRECTION AND RELATIVE RATE OF FLOW (SEEBECK ET AL. 2014).

The three dimensional model of Seebeck et al. (2014) can be analysed in cross section through the fault as a series of high and low permeability zones that have associated fluxes and fracture densities. Figure 31 shows a schematic distribution of hydrogeological properties for a complicated fault zone architecture (after Faulkner et al., 2010) where: “(a) is a single high strain slip zone surrounded by a lower strain damage zone (e.g. Chester and Logan, 1986); (b) is an anastomosing pattern of multiple high strain slip zones bounding variably strained protolith (e.g. Wallace and Morris, 1986). The bulk physical properties of these two end-members is dependent on the scale of observation. A critical fracture density (C_f) is required before macro-scale permeability occurs. Fault zone architecture is comprised of four main elements; 1) Fault rock (gouge, breccia, cataclasite), 2) Fault bound lenses of variably strained wall rock, 3) Fractured wall rock and 4) Protolith. Filled blue circles indicate locations of water flow”.

The complex distribution of permeability and flux associated with fault zone architecture and supported by field data described by Seebeck et al. (2013) is mainly related to basement rheologies, however it compliments similar concepts described by Bense et al. (2013) and highlights the challenges of characterising fault zone hydraulic properties in regional groundwater flow models. In many cases detailed nested models may be required to understand key hydraulic processes that can then be used to upscale certain properties to regional scale groundwater flow models. Traditional approaches of examining hydrocarbon systems that have either been sealed or not by fault zones provide an interesting estimate of bulk fault zone hydraulic properties. The differences between these two scales may be related to the nature of the damage zone as a fault crosses top seal lithology that has more ductile rock physics properties. In other words, the required detail to which fault zone hydraulic properties should be scaled up may be host rock specific.

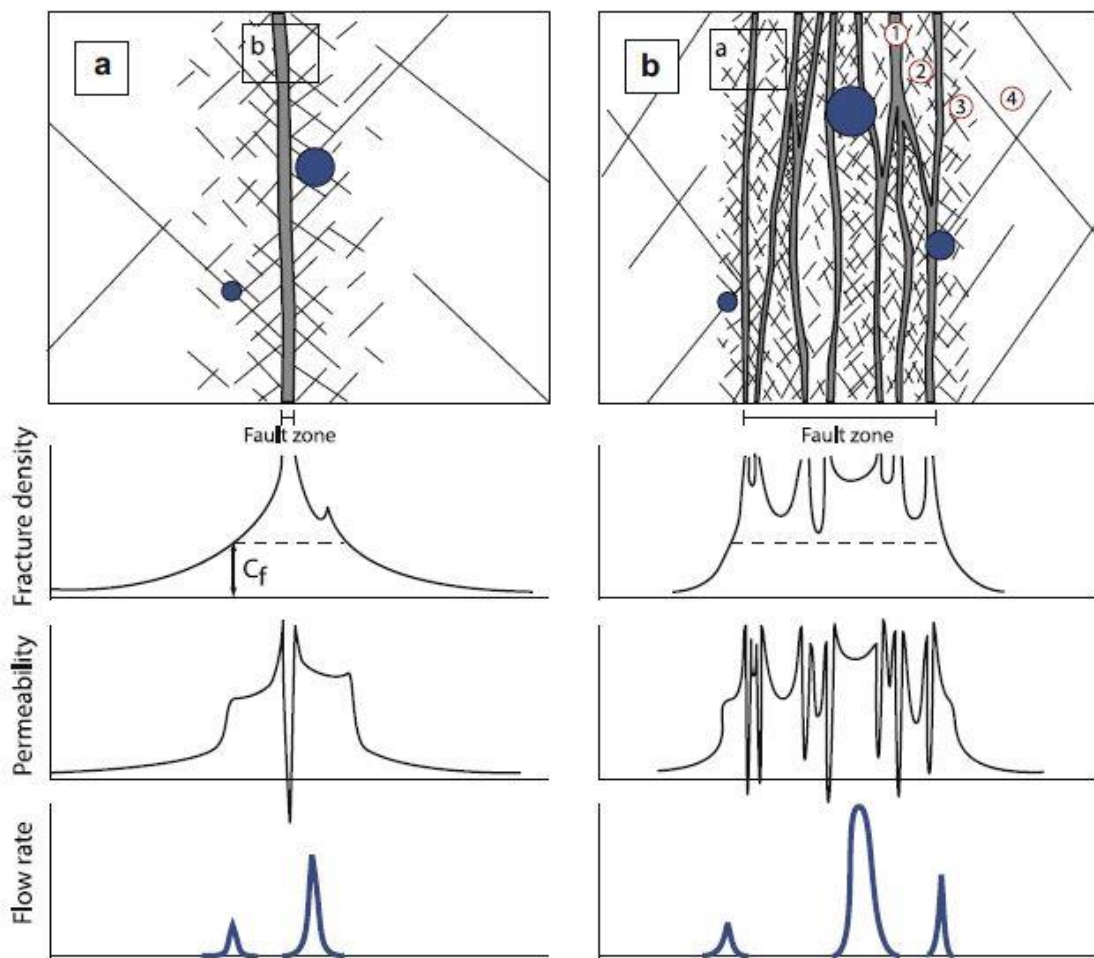


FIGURE 31. FLUID FLOW IN FAULT ZONES FROM AN ACTIVE RIFT. GEOMETRY OF THE DETAILED FAULT ZONE ARCHITECTURE RELATED TO THE FRACTURE DENSITY, PERMEABILITY AND FLUX DISTRIBUTION OF FORMATION WATER (SEEBECK ET AL. 2014).

10 Discussion and Summary of Fault Assessment, Sealing Capacity and Reactivation Potential

It should be noted that our understanding of how faults initiate and develop is to a large extent based on literature where faults in basement have been studied. Some researchers have tried to apply this to faults in siliciclastic strata but there is no clear agreement if this is appropriate or not (e.g. Figure 32). It is clear that the detailed fault zone architecture is influenced by the rheology of the host rock and by pre-existing planes of weakness. There is also a depth relationship with rheology that is associated with temperature and pressure. This extends from the shallow unconsolidated to the intermediate brittle and finally the deep ductile domains. For example, this can influence the extent to which a fault damage zone might extend outwards from the fault plane core. The tectonic and burial history are also important as the current depth of faults may not be representative of the depth at which the fault was initially formed. In a sedimentary pile with observable faults one might be able to discern the degree and extent of a damage zone by examining wellbore image logs and characterising fracture density as a function of proximity to the identified fault zone.

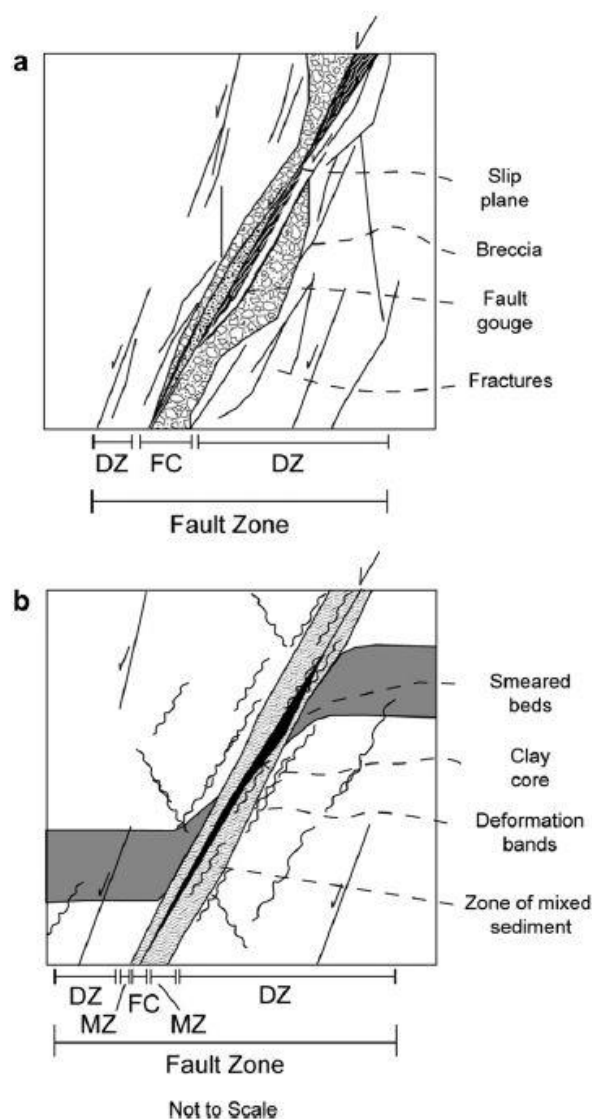


FIGURE 32. TYPICAL ARCHITECTURAL AND STRUCTURAL ELEMENTS OF FAULT ZONES (LOVELESS ET AL. 2011). A) FAULT ZONE IN CRYSTALLINE ROCKS (E.G. CAINE ET AL., 1996) WITH A FAULT CORE (FC) AND DAMAGE ZONE (DZ). B) FAULT ZONE IN POORLY LITHIFIED SEDIMENT (E.G. HEYNEKAMP ET AL., 1999; RAWLING AND GOODWIN, 2003; RAWLING AND GOODWIN, 2006), THE MIXED ZONE (MZ) IS A THIRD ARCHITECTURAL ELEMENT.

Once a fault has been initiated within a rock matrix, it is clear that further strain is often preferentially localised on certain parts of the existing structures resulting in a wide range of transient strain accumulation across a population of faults and fractures. Often there are patterns to the spatial distribution of observed fault zone size distribution and this may allow for the prediction of other faults and fractures yet to be identified. In the historic literature there is often a tendency for a particular type of strain mode to be “popular” at the time and this can influence the style of faulting interpreted from seismic and outcrop data. For example a, strike-slip component to fault displacement for very long coalesced fault planes was a commonly favoured interpretation for certain periods while recently the interpretation of relay ramps is often invoked.

From this literature review and assessment of commonly used fault analysis methodology, we collected several case study examples of fault systems and their hydraulic behaviour and make the following general observations:

- Faults can exhibit the full range of hydraulic characteristics between providing a hydraulic barrier sufficient to trap hydrocarbons for millions of years to being a conduit with transmissivities capable of transmitting groundwater from depth to surface thermal springs;
- Faults can exhibit different hydraulic properties at different locations on the fault plane;
- The hydraulic behaviour exhibited by faults is related to a combination of: 1) the geometry or architecture of the fault complex, 2) the rheology of the host rocks that the fault plane crosses, and 3) the distribution and orientation of in situ stress;
- Faults occur in predictable populations representing a power law distribution of fault size (or throw). The observed strain together with the predicted fault size distribution can be used to estimate the unobserved (sub-seismic) strain;
- In scenarios of coal seam gas development where the formation pressure is reduced regionally over time by groundwater abstraction associated with gas production, there is an associated change in the effective stress and thus potential for a change in the sealing properties of faults. Coupled geomechanical and hydrodynamic processes are required to characterise these transient processes;
- Fault hydraulic properties can depend on the environmental conditions (pressure, temperature, depth and stress) both at the time the fault formed and the present day; and
- Observations of springs occurring along faults including spring discharge flux, temperature and geochemistry can be used to calibrate and validate the hydraulic characteristics estimated for fault zones.

11 Implications for up-scaling to Regional Groundwater Models

Concerns of aquifer pressure depletion, fugitive methane migration and degradation of aquifer water quality due to CSG development effects propagating up faults can be investigated through the use of regional groundwater models, if they are appropriately parameterised. A key aspect of this investigative approach is to develop and parameterise regional groundwater models that accurately represent the properties of the rock framework and its contained fluids. In this review we consider methodologies for estimating the properties of faults and how these can be represented in regional groundwater models. There are a number of key parameters and processes that need to be assessed at a detailed scale and then up-scaled for parameterisation of regional models. For the incorporation of fault properties these include:

- Details of the host rock facies distributions and lithologies;
- Details of the fault throw distributions;
- Details of the in situ stress distribution;
- Details of the fault zone damage zone distribution and fault core distribution;
- Details of the mechanical strength of the fault plane and damage zone;
- Details of the host rock rheology, depth, temperature and how these relate to the tectonic and burial history (this is important for both the aquifer and aquitard layers transected by the fault);
- Details of the fluid pressure distribution in both the aquifers and aquitards on either side of the fault;
- Details of the various fluid types, densities, surface tensions and wettabilities;
- Details of other supporting fluid data such as formation water chemistry and formation temperature;

- Details of the transient nature of predicted reservoir and adjacent aquifer pressure depletion that could impact the effective stress; and
- Well characterised analogues from outcrop or sub-surface features that can be used to interpolate key characteristics not well enough constrained by data at the site location of interest.

This review provides the framework that can be used to guide research (the next stage of work after this review) into appropriate methodologies and procedures of fault zone hydraulic characterization applied to regional groundwater models.

12 References

- Ackermann, R.V., Schlische, R.W. and Withjack, M.O., 2001. The geometric and statistical evolution of normal fault systems: An experimental study of the effects of mechanical layer thickness on scaling laws. *Journal of Structural Geology*. 23, 1803–1819.
- Allan, U.S., 1989. Model for hydrocarbon migration and entrapment within faulted structures. *American Association of Petroleum Geologists Bulletin*. 73 (7), 803-811.
- Apourvari, S. N., and Arns, C. H., 2016. Image-based relative permeability upscaling from the pore scale. *Advances in Water Resources*.
- Bachu, S., 1995. Flow of variable-density formation water in deep sloping aquifers: review of methods of representation with case studies: *Journal of Hydrology*. 164, 19-38.
- Bachu, S. and Burwash, R.A., 1991. Regional-scale analysis of the geothermal regime in the Western Canada Sedimentary Basin, *Geothermics*. 20, 387-407.
- Bachu, S., Ramon, J.C., Villegas, M.E. and Underschlutz, J.R., 1995. Geothermal regime and thermal history of the Llanos Basin, Colombia: *American Association of Petroleum Geologists Bulletin*. 79 (1), 116-129.
- Bachu, S. and Michael, K., 2002. Flow of variable-density formation water in deep sloping aquifers: minimizing the error in representation and analysis when using hydraulic head distributions. *Journal of Hydrology*. 259, 49-65.
- Bailey, W.R., Underschlutz J., Dewhurst D.N., Kovack G., Mildren S. and Raven M., 2006. Multi-disciplinary approach to fault and top seal appraisal; Pyrenees-Macedon oil and gas fields, Exmouth Sub-basin, Australian Northwest Shelf. *Marine and Petroleum Geology*. 23, 241-259.
- Bense, V.F., 2004. The hydraulic properties of faults in unconsolidated sediments and their impact on groundwater flow. PhD Thesis. Vrije University Amsterdam. 143 p.
- Bense, V.F. and Van Balen, R., 2004. The effect of fault relay and clay smearing on groundwater flow patterns in the Lower Rhine Embayment. *Basin Research*. 16, 397–411.
- Bense, V.F. Gleeson, T. Loveless, S.E. Bour, O. and Scibek, J., 2013. Fault zone hydrogeology. *Earth-Science Reviews*. 127, 171–192
- Bjørkum P.A., Walderhaug O. and Nadeau, P.H., 1998. Physical constraints on hydrocarbon leakage and trapping revisited: *Petroleum Geoscience*. 4, 237-239.
- Bourne, S.J. and Willemse, E.J.M., 2001. Elastic stress control on the pattern of tensile fracturing around a small fault network at Nash Point, UK. *Journal of Structural Geology*. 23, 1753–1770.
- Bourne, S.J., Rijkels, L., Stephenson, B.J. and Willemse, E.J.M., 2001. Predictive modelling of naturally fractured reservoirs using geomechanics and flow simulation. *Georabia*. 6, 27–42.
- Bouvier, J.D., Kaars-Sijpesteijn, C.H., Kluesner, D.F., Onyejekwe, C.C. and R.C. van der Pal, 1989. Three-dimensional seismic interpretation and fault sealing investigations, Nun River Field, Nigeria: *American Association of Petroleum Geologists Bulletin*. 73, 1397-1414.
- Bretan, P., Yielding, G. and Jones, H., 2003. Using calibrated shale gouge ratio to estimate hydrocarbon column heights. *American Association of Petroleum Geologists Bulletin*. 87, 397-413.
- Brooks, R.H. and Corey, A., 1966. Properties of porous media affecting fluid flow. *Journal of the Irrigation and Drainage Division*. 92, (2), 61-90.

- Brown, A., 2003. Capillary effects on fault-fill sealing. *American Association of Petroleum Geologists Bulletin*. 87, 381-395.
- Ciftci, N.B. and Bozkurt, E., 2007. Anomalous stress field and active breaching at relay ramps: a field example from Gediz Graben, SW Turkey. *Geol Mag.* 144 (4) 687-699.
- CH2MHill, 2013. Water Resources MNES: PEL238 Cumulative Groundwater Impact Assessment. Energy NSW Coal Seam Gas Exploration and Appraisal Program, Referral of Proposed Action: Water Resources Assessment, Gunnedah Basin NSW. 33 p.
- Chester, F.M. and Logan, J.M., 1986. Implications for mechanical properties of brittle faults from observations of the Punchbowl Fault Zone, California. *Geophys.* 124 (1/2), 79-106.
- Caine, J.S., Evans, J.P. and Forster, C.B., 1996. Fault zone architecture and permeability structure. *Geology* 24 (11), 1025-1028.
- Clayton, C.J., 1999. Discussion: 'Physical constraints on hydrocarbon leakage and trapping revisited' by Bjørkum et al.: *Petroleum Geoscience*. 5, 99-101.
- Corey, A.T., 1954. The interrelation between gas and oil relative permeabilities. *Producers Monthly*. 19, (1), 38-41.
- Cowley, R. and O'Brien, G.W., 2000. Identification and interpretation of leaking hydrocarbons using seismic data: A comparative montage of examples from major fields in Australia's North West Shelf and Gippsland Basin. *Australian Petroleum Production and Exploration Association Journal*. 40, (1), pp. 121-150.
- Craw, D., 2000. Fluid flow at fault intersections in an active oblique collision zone, Southern Alps, New Zealand. *Journal of Geochemical Exploration*. 69 and 70, 523-526.
- Dahlberg, E.C., 1995. *Applied hydrodynamics in petroleum exploration*, second edition. Springer-Verlag New York Inc., 295 p.
- Dee, S.J., Yielding, G., Freeman, B., Healy, D., Kuszniir, N.J., Grant, N. and Ellis, P., 2007. Elastic dislocation modelling for prediction of small-scale fault and fracture network characteristics. In Lonergan, L., Jolly, R.J.H., Rawnsley, K. and Sanderson, D.J. (Eds) *Fractured Reservoirs*. Geological Society of London, Special Publications. 270, 139-155.
- Di Bucci, D., Massa, B., and Zuppetta, A., 2006. Relay ramps in active normal fault zones: A clue to the identification of seismogenic sources (1688 Sannio earthquake, Italy). *Geological Society of America Bulletin*. 118, (3/4), 430-448; doi: 10.1130/B25783.1
- Donaldson, E.C., and Alam, W., 2013. *Wettability*: Elsevier. 336 p.
- Faulkner, D.R., Jackson, C.A.L., Lunn, R.J., Schlische, R.W., Shipton, Z.K., Wibberley, C.A.J. and Withjack, M.O., 2010. A review of recent developments concerning the structure, mechanics and fluid flow properties of fault zones. *Journal of Structural Geology*. 32, 1557-1575.
- Fensham, R., Esterle, J., Vink, S., Wolhuter, A., Silcock, J., Hines, K., and Drimer, J., 2014. Ecological and hydrogeological survey of the Great Artesian Basin springs - Springsure, Eulo, Bourke and Bogan River supergroups, Volume 1: history, ecology and hydrogeology: Department of the Environment, Commonwealth of Australia. 275 p.
- Fulljames, J.R., Zijerveld, L.J.J., and R.C.M.W. Franssen, 1997. Fault seal processes: systematic analysis of fault seals over geological and production timescales. In: Moller-Pedersen, P. and A.G. Koestler (eds), *Hydrocarbon Seals: Importance for Exploration and Production*. Norwegian Petroleum Society (NPF), Special publication 7. Elsevier, Amsterdam, 51-59.

Gartrell, A., Lisk, M. and Undershultz, J., 2002. Controls on the trap integrity of the Skua Oil Field, Timor Sea. *In*: Keep, M. and Moss, S. J. (eds.), *The Sedimentary Basins of Western Australia 3: Proceedings of Petroleum Exploration Society of Australia*, 390-407.

Gartrell, A., Zhang, Y., Lisk, M. and Dewhurst, D., 2004. Fault intersections as critical hydrocarbon leakage zones: Numerical modelling as an example from the Timor Sea, Australia. *Marine and Petroleum Geology*. 21, 1165-1179.

Gartrell, A., Bailey, W., Brincat, M. and Underschultz, J., 2005. Strain localisation and trap geometry as key controls on hydrocarbon preservation in the Laminaria High area. *APPEA Journal*. 45, (1), 477-492.

Gartrell, A., Bailey, W.M. and Brincat, M., 2006. A new model for assessing trap integrity and oil preservation risks associated with post-rift fault reactivation in the Timor Sea. *The American Association of Petroleum Geologists Bulletin*. 90, (12), 1921-1944.

Gibson, R.G., 1998, Physical character and fluid-flow properties of sandstone-derived fault zones. *In*: Coward, M.P., Daltaban, T.S., and Johnson, H., (eds.) *Structural Geology in Reservoir Characterisation*. Geological Society of London, Special Publications. 127, 83-97.

Gillespie, P.A., Howard, C.B., Walsh, J.J and Watterson, J., 1993. Measurement and characterisation of spatial distributions of fractures. *Tectonophysics*. 226, (1), 113-141.

Grasby, S.E. and Hutcheon, I., 2001. Controls on the distribution of thermal springs in the southern Canadian Cordillera. *Canadian Journal of Earth Sciences*. 38, (3), 427-440. doi: 10.1139/e00-091

Gudmundsson, A., 2000. Active fault zones and groundwater flow. *Geophysical Research Letters*. 27, (18), 2993-2996. doi: 10.1029/1999gl011266

Habermehl, M.A., 1982. Springs in the Great Artesian Basin, Australia - Their Origin and Nature. Canberra: Department of National Development and Energy. 54 p.

Heller, R., Vermeylen, J., Zoback, M., 2014. Experimental investigation of matrix permeability of gas shales. *The American Association of Petroleum Geology Bulletin*. 98, (5), 975-995.

Herring, A. L., Andersson, L., Schlüter, S., Sheppard, A., and Wildenschild, D., 2015. Efficiently engineering pore-scale processes: The role of force dominance and topology during nonwetting phase trapping in porous media. *Advances in Water Resources*, 79, 91-102.

Heum, O.R., 1996. A fluid dynamic classification of hydrocarbon entrapment. *Petroleum Geoscience*. 2, 145-158.

Heynekamp, M.R., Goodwin, L.B., Mozley, P.S. and Haneberg, W.C., 1999. Controls on fault-zone architecture in poorly lithified sediments, Rio Grande Rift, New Mexico: Implications for fault zone permeability and fluid flow. *In*: Haneberg, P.S., Mozley, P.S., Moore, J.C. and Goodwin, L.B. (Eds.), *Faults and Subsurface Fluid Flow in the Shallow Crust*. American Geophysical Union Monograph. 113, 27-49.

Hitchon, B., and Brulotte, M., 1994. Culling criteria for "standard" formation water analyses: Applied Geochemistry. 9, 637-645.

Iglauer, S., Pentland, C., and Busch, A., 2015. CO₂ wettability of seal and reservoir rocks and the implications for carbon geo-sequestration. *Water Resources Research*, 51(1), 729-774.

Jaeger, J.C. and Cook, N.G.W., 1979. *Fundamentals of rock mechanics*. Chapman & Hall, New York, 76 p.

Josh M., Esteban, L., Delle Piane, C., Sarout, J., Dewhurst, D.N., & Clennell, M.B., 2012. Laboratory characterisation of shale properties. *Journal of Petroleum Science and Engineering*. 88-89, 107-124.

- Keppel, M., Karlstrom, K.E., Love, A.J., Priestley, S., Wohling, D., and Ritter, S.D., 2013. Allocating water and maintaining springs in the Great Artesian Basin, Volume 1: Hydrogeological Framework of the Western Great Artesian Basin (Vol. 1). Canberra: National Water Commission. 50 p.
- Kim, Y.S., and Sanderson, D.J., 2005. The relationship between displacement and length of faults: a review. *Earth-Science Reviews*. 68, (3–4), 317–334.
- Krause, M. H., and Benson, S. M., 2015. Accurate determination of characteristic relative permeability curves. *Advances in Water Resources*, 83, 376–388.
- Langhi, L., Zhang, Y., Gartrell, A., Underschultz J.R. and Dewhurst. D.N., 2009. Fluid flow behaviour in reactivated hydrocarbon traps: assessing fluid circulation along natural complex fault systems using numerical fluid flow simulation. *Journal of Geochemical Exploration*. 101, (1), 57–57. ISSN: 03756742.
- Langhi, L., Zhang, Y., Gartrell, A., Underschultz, J., and Dewhurst, D., 2010. Evaluating hydrocarbon trap integrity during fault reactivation using geomechanical three dimensional modeling: An example from the Timor Sea, Australia. *The American Association of Petroleum Geology Bulletin*. 94, (4), 567–591.
- Langhi, L., Ciftci, B. and Strand, J., 2013. Fault seal first order analysis: SW Hub. CSIRO report EP13879, open file. 60 p.
- Lindsay, N.G., Murphy, F.C., Walsh, J.J. and Watterson, J., 1993. Outcrop studies of shale smear on fault surfaces: Special Publication, International Association of Sedimentologists. 15, 113–123.
- Lopez, D.L., and Smith, L., 1995. Fluid flow in fault zones: Analysis of the interplay of convective circulation and topographically driven groundwater flow. *Water Resources Research*. 31, (6), 1489–1503.
- Loveless, S., Bense, V., and Turner J., 2011. Fault architecture and deformation processes within poorly lithified rift sediments, Central Greece. *Journal of Structural Geology*. 33, (11), 1554–1568.
- Maerten, L., Gillespie, P. and Pollard, D.D., 2002. Effects of local stress perturbation on secondary fault development. *Journal of Structural Geology*. 24, (1), 145–153.
- Manzocchi, T., Walsh, J.J. and Bailey, W.R., 2009. Population scaling biases in map samples of power-law fault systems. *Journal of Structural Geology*. 31, (12) 1612–1626.
- Manzocchi, T. and Childs, C., 2013. Quantification of hydrodynamic effects on capillary seal capacity. *Petroleum Geoscience*. 19, 105–121.
- Meyer, V., Nicol, A., Childs, C., Walsh, J.J. and Watterson, J., 2002. Progressive localisation of strain during the evolution of a normal fault system. *Journal of Structural Geology*. 24, (8), 1215–1231.
- Mildren, S.D., Hillis, R.R. and Kaldi, J.G., 2002. Calibrating predictions of fault seal reactivation in the Timor Sea. *Australian Petroleum Production & Exploration Association Journal*. 42, (1), 187–202.
- Mildren, S.D. and Hillis, R.R., 2002. FAST: A new approach to risking fault reactivation and related seal breach. Paper presented at the AAPG Hedberg Research Conference, Borossa Valley, South Australia.
- Moria, S., 2011. Effective permeability to water in petroleum column from capillary pressure data: implications for hydrodynamic effects on capillary seal capacity. *Petroleum Geoscience*. 17, 397–404.
- Neele, F., ten Veen, J., Wilschut, F. and Hofstee, C., 2012. Independent assessment of high-capacity offshore CO₂ storage options. TNO report TNO-060-UT-2012-00414. 85p.
- Okada, Y., 1992. Internal deformation due to shear and tensile faults in a half-space. *Bulletin of The Seismological Society Of America*. 82, 1018–1040.

- Otto, C., Underschultz, J., Hennig, A. and V. Roy, 2001. Hydrodynamic analysis of flow systems and fault seal integrity in the Northwest Shelf of Australia. *APPEA Journal*. 41, 347-365.
- Peacock, D.C.P. and Sanderson, P., 1994. Geometry and development of relay ramps in normal fault systems. *The American Association of Petroleum Geologists Bulletin*. 78, (2), 147-165.
- Pini R., and Benson, S.M., 2013. Simultaneous determination of capillary pressure and relative permeability curves from core-flooding experiments with various fluid pairs. *Water Resources Research*. 49, (6), 3516-3530.
- Pini, R., and Benson, S. M., 2015. Quantifying Hydrogeological Heterogeneity of Rocks using Core-Floods. *Pore Scale Phenomena: Frontiers in Energy and Environment* (pp. 243-261): World Scientific.
- Queensland-Water-Commission, 2012. Underground water impact report. Brisbane: Queensland Water Commission. 224 p.
- Rawling, G.C. and Goodwin, L.B., 2003. Cataclasis and particulate flow in faulted, poorly consolidated sediments. *Journal of Structural Geology*. 25, (3), 317-331.
- Rawling, G.C. and Goodwin, L.B., 2006. Structural record of the mechanical evolution of mixed zones in poorly lithified sediments, Rio Grande rift, New Mexico, USA. *Journal of Structural Geology*. 28, (9), 1623-1639.
- Rodgers S., 1999. Discussion: 'Physical constraints on hydrocarbon leakage and trapping revisited' by Bjørkum et al. – further aspects: *Petroleum Geoscience*. 5, 421-423.
- Seebeck, H., Nicol, A., Walsh, J.J., Childs, C., Beetham, R.D. and Pettinga, J., 2014. Fluid flow in fault zones from an active rift: *Journal of Structural Geology*, 62, 52-64.
- Sorkhabi, R., 2013. Know your faults! Part II. *GeoExPro*. 9, (6), 72-86.
- Sperrevik, S., Gillespie, P.A., Fisher, Q.J., Halvorsen, T. and Knipe, R.J., 2002. Empirical estimation of fault rock properties. *In*: Koestler, A.G. and R. Hunsdale, (eds). *Hydrocarbon Seal Quantification*, NPF Special Publication. 11, 109-125. Elsevier, Amsterdam.
- Talukder, A.R., Ross, A., Crooke, E., Stalvies, C., Trefry, C. and Qi, X., 2013. Natural hydrocarbon seepage on the continental slope to the east of Mississippi Canyon in the northern Gulf of Mexico. *Geochemistry Geophysics Geosystems*. 14, (6), 1940-1956.
- Teige, G.M.G., Hermanrud, C., Thomas, W.H., Wilson, O.B. and Bolas H.M.N., 2005. Capillary resistance and trapping of hydrocarbons: a laboratory experiment: *Petroleum Geoscience*, 11, 125-129.
- Teige, G.M.G., Thomas, W.L.H., Hermanrud, C., Øren, P., Rennan, L., Wilson, O.B. and Bolås H.M.N., 2006. Relative permeability to wetting-phase water in oil reservoirs. *Journal of Geophysical Research*. 111, (B12), B12204.
- Underschultz, J., 2005. Pressure distribution in a reservoir affected by capillarity and hydrodynamic drive: Griffin Field, North West Shelf, Australia. *Geofluids Journal*. 5, 221-235.
- Underschultz, J.R., 2007. Hydrodynamics and membrane seal capacity. *Geofluids Journal*. 7, 148-158.
- Underschultz, J.R., Ellis, G., Hennig, A., Bekele E. and Otto. C., 2002. Estimating formation water salinity from wireline pressure data, case study in the Vulcan Sub-Basin. *Petroleum Exploration Society of Australia. The sedimentary basins of Western Australia III: proceedings of the Western Australian Basins Symposium (WABS) III*. 285-303.
- Underschultz, J.R., Otto C.J. and Cruse, T., 2003. Hydrodynamics to assess hydrocarbon migration in faulted strata - methodology and a case study from the Northwest Shelf of Australia. *Journal of Geochemical Exploration*. 78-79, 469-474.

Underschultz, J.R., Otto, C.J. and Bartlett, R., 2005. Formation fluids in faulted aquifers; Examples from the foothills of Western Canada and the North West Shelf of Australia. In (P, Boulton and J. Kaldi, eds.) Evaluating fault and cap rock seals, The American Association of Petroleum Geologists Hedberg Series. No 2, 247-260

Underschultz, J.R. and Strand, J., (2016). Capillary seal capacity of faults under hydrodynamic conditions. *Geofluids Journal*. DOI: 10.1111/gfl.12166.

Wallace, R.E. and Morris, H.T., 1986. Characteristics of faults and shear zones in deep mines. *Geophys.* 124, (1/2), 105-125.

Walsh, J.J. and Watterson, J., 1988. Analysis of the relationship between displacements and dimensions of faults. *Journal of Structural Geology*. 10, (3), 239-247.

Watterson, J., Nicol, A. and Walsh, J.J., 1998. Strains at the intersections of synchronous conjugate normal faults. *Journal of Structural Geology*. 20, (4), 363-370.

Watts, N.L., 1987. Theoretical aspects of cap-rock and fault seals for single and two-phase hydrocarbon columns. *Marine and Petroleum Geology*. 4, 274-307.

Yassir, N. and Otto, C.J., 1997. Hydrodynamics and fault seal assessment in the Vulcan Subbasin, Timor Sea. *Australian Petroleum Production and Exploration Association Journal*. 37, (1), 380-389.

Yielding, G., 2002. Shale gouge ratio – Calibration by geohistory. *In*: Koestler, A.G. and Hunsdale (eds.), *Hydrocarbon Seal Quantification*: Amsterdam, Elsevier, Norwegian Petroleum Society (NPF) Special Publication. 11, 1-15.

Yielding, G., Needham, T. and Jones, H., 1996. Sampling of fault populations using sub-surface data: A review. *Journal of Structural Geology*. 18, (2–3), 135-146.

Yielding, G., Freeman, B., and D.T. Needham, 1997. Quantitative fault seal prediction: The American Association of Petroleum Geology Bulletin. 81, 897-917.

Yielding G., Bretan, P. and Freeman, B., 2010. Fault seal calibration: a brief review. *Geological Society, London, Special Publications*. 347, 243-255.

Zhang, Y., Gartrell, A., Underschultz, J.R. and Dewhurst, D.N., 2009. Numerical modelling of strain localisation and fluid flow during extensional fault reactivation: implications for hydrocarbon preservation. *Journal of Structural Geology*. 31, (3), 315-327.

Zhang, Y., Underschultz, J.R., Gartrell, A., Dewhurst, D.N., and Langhi, L., 2011. Effects of regional fluid pressure gradients on strain localisation and fluid flow during extensional fault reactivation. *Marine and Petroleum Geology*. 28, (9), 1703-1713. doi: 10.1016/j.marpetgeo.2011.07.006